Title: TOR signaling regulates GPCR levels on the plasma membrane and suppresses the *Saccharomyces cerevisiae* mating pathway

Authors: Nicholas R. Leclerc[1], Toby M. Dunne[1], Sudati Shrestha[1], Cory P. Johnson[2], Joshua B. Kelley[1,2*]

Affiliations:

[1]Department of Molecular and Biomedical Sciences, University of Maine; Orono, USA.

[2]Graduate School of Biomedical Science and Engineering, University of Maine; Orono, USA.

*Corresponding author. Email: joshua.b.kelley@maine.edu

Abstract:

Saccharomyces cerevisiae respond to mating pheromone through the GPCRs Ste2 and Ste3, which promote growth of a mating projection in response to ligand binding. This commitment to mating is nutritionally and energetically taxing, and so we hypothesized that the cell may suppress mating signaling during starvation. We set out to investigate negative regulators of the mating pathway in nutritionally depleted environments. Here, we report that nutrient deprivation led to loss of Ste2 from the plasma membrane. Recapitulating this effect with nitrogen starvation led us to hypothesize that it was due to TORC1 signaling. Rapamycin inhibition of TORC1 impacted membrane levels of all yeast GPCRs. Inhibition of TORC1 also dampened mating pathway output. Deletion analysis revealed that TORC1 repression leads to α-arrestin-directed CME through TORC2-Ypk1 signaling. We then set out to determine whether major downstream effectors of the TOR complexes also downregulate pathway output during mating. We found that autophagy contributes to pathway downregulation through analysis of strains lacking *ATG8*. We also show that Ypk1 significantly reduced pathway output. Thus, both autophagy machinery and TORC2-Ypk1 signaling serve as attenuators of pheromone signaling during mating. Altogether, we demonstrate that the stress-responsive TOR complexes coordinate GPCR endocytosis and reduce the magnitude of pheromone signaling, in ligand-independent and ligand-dependent contexts.

One Sentence Summary:

TOR signaling regulates the localization of all *Saccharomyces cerevisiae* GPCRs during starvation and suppress the mating pathway in the presence and absence of ligand.

Main Text:

INTRODUCTION

G-protein-coupled receptors (GPCRs) are a conserved family of eukaryotic membrane proteins that serve as sensors of the extracellular environment (*1, 2*). GPCRs are functionally unique from other cell surface receptors due to their coupling with a heterotrimeric G-protein (consisting of Gα, Gβ, and Gγ subunits) (*3*). This large G-protein facilitates signal transduction from an active receptor to downstream effectors, including adenylate cyclase (*4*), phospholipase C (*5*), phosphoinositide 3-kinases (PI3K) (*6*), mitogen-activated protein kinases (*7*), and more (*8*).

GPCRs are central to cell communication in the human body, and as such, are a primary target of FDA-approved drugs (~34%) (*9*). GPCR signaling must be tightly regulated to prevent maladaptation to extracellular cues. Prolonged signaling of GPCRs results in deleterious outcomes, including heart failure (*10*), cell death, and uncontrolled proliferation (*11, 12*). To prevent these consequences, cells attenuate GPCR signaling primarily through two approaches: 1) receptor endocytosis (*13, 14*) and 2) negative regulation by a Regulator of G-protein Signaling (RGS) (*15-17*).

RGS proteins are a family of GTPase-activating proteins (GAP) that catalyze the inactivation of Gα subunits (*18*). Upon GPCR activation, Gα and Gβγ subunits will dissociate from each other, allowing for Gα to exchange its bound GDP for GTP and assume an active conformation (*19*). RGS proteins will associate with active GTP-bound Gα and facilitate their intrinsic GTPase activity, thereby cleaving GTP to GDP. In-turn this produces an inactive GDP-bound Gα subunit, causing it to re-associate with Gβγ and repress its signaling (*18, 20, 21*). This Gα-specific GAP activity is hallmark of RGS proteins and is conserved among eukaryotes (*22-24*). Receptor endocytosis is also a conserved mechanism of GPCR downregulation in eukaryotes (*12-14, 25*). Ligand detection by a GPCR causes it to change its conformation such that its cytosolic C-terminus is susceptible to post-translational modification (PTM) including phosphorylation and ubiquitination (*26, 27*). The cytosolic tail of the receptor is phosphorylated by G-protein Receptor Kinases (GRK) following GPCR activation, leading to β-arrestin recruitment (*28, 29*). β-arrestins facilitate endocytosis of GPCRs (*30*), leading to their downregulation (*31*). Although, GPCR downregulation may be short- or long-term depending on the events following internalization (*12*). Phosphorylation of the GPCR C-terminus leads to receptor internalization to an endosomal compartment, thereby uncoupling the receptor from the G-protein to promote acute desensitization (*32, 33*). This is typically a short-term downregulatory process because GPCRs may be re-sensitized at the endosome and recycled back to the plasma membrane (PM) (*14, 34-36*). In contrast, active GPCRs that are also ubiquitinated are internalized and often trafficked to the lysosome to be degraded (*37, 38*). In this context, the destruction of the GPCR leads to a long-term downregulation of its signaling (*12*). These scenarios seem to paint a picture where receptor endocytosis always leads to signal attenuation. However, there is an expanding knowledgebase that suggests that internalized GPCRs may continue to signal from the endomembrane system to produce unique signaling profiles that still requires thorough characterization (*39-42*). Nevertheless, endocytosis is still a significant negative-regulator of GPCR signaling systems throughout eukaryotes, including the mating pathway of *Saccharomyces cerevisiae (25)*.

S. cerevisiae haploids exist in two mating types, MAT**a** and MATα. These cells secrete mating pheromones depending on their type: MAT**a** cells secrete **a**-factor, and MATα cells secrete α-factor (*43-45*). Cells recognize mating pheromone of the opposite type through their mating GPCRs: Ste2 in MAT**a** (*46*)**,** and Ste3 in MATα (*47*). This initiates an identical signaling cascade resulting in polarized growth, cell cycle arrest in G1, and transcription of mating genes. Through this GPCR-mediated response, cells are primed to form a mating projection toward the source of pheromone, fuse, and mate with the nearest available partner of the opposite mating type (*43-45*). In the case that multiple cells attempt to mate with the same potential partner, only one can complete the mating process (*48*). Prolonged signaling through Ste2 and Ste3 can lead to cell death (*49*), and so it is important that cells negatively regulate mating signaling and return to mitosis. Yeast have three primary negative regulators of the mating pathway: 1) RGS activity (*50, 51*), 2) degradation of α-factor pheromone by the protease Bar1 (*52, 53*), and 3) endocytosis

of the mating receptor (*25*). These processes desensitize the cell to pheromone at the ligand, receptor, and G-protein level, downregulating the mating pathway and preventing further pheromone signaling.

Receptor endocytosis of Ste2 and Ste3 has been thoroughly characterized in *S. cerevisiae*. While yeast share many mechanistic aspects of receptor endocytosis to mammals, they also are unique. GPCR activation results in C-terminal phosphorylation by Yeast Casein Kinases (Yck1 and Yck2) (*54-56*), unlike mammalian GPCRs that are phosphorylated by GRKs (*57, 58*). Phosphorylation allows for the recruitment of α-arrestins (Rod1 and Rog3) (*25, 59*), rather than β-arrestins. Following recruitment of α-arrestins, the receptor tail is multi-monoubiquitinated (*60*), allowing for recruitment of epsin-like proteins (Ent1 and Ent2) that recruit endocytic machinery (*61, 62*) and promote internalization of the receptor (*63, 64*). Following receptor-mediated endocytosis, Ste2 is trafficked to the vacuole (lysosome) for degradation (*65, 66*), whereas Ste3 localizes at the endosome and is recycled (*67*). Both of these scenarios lead to the desensitization of the mating receptors to pheromone (*25, 68*).

The central metabolic regulator Target of Rapamycin (TOR) kinase is conserved across eukaryotes (*69*). TOR kinases were first discovered in yeast as Tor1 and Tor2 (*70, 71*). Subsequently, the mammalian mTOR was identified with highly conserved mechanisms of action (*72-75*). Tor kinases assemble into two distinct protein complexes, TORC1 and TORC2 (mTORC1 and mTORC2 in mammals) (*76*). These complexes each function as Ser/Thr kinases (*77*) that regulate metabolism, growth, autophagy, and endocytosis in response to various stressors (*78, 79*). While mammalian cells harbor one mTOR protein that assembles into either complex, *S. cerevisiae* have two, Tor1 and Tor2 (*76*). This is likely due to whole genome duplication, a significant evolutionary event that led to the generation of multiple copies of pre-existing proteins (*80*). While Tor1 assembles into TORC1, Tor2 may assemble into both TORC1 and TORC2 (*76, 81*). TORC1 resides in the perivacuolar space (*82*) and is primarily responsive to available nutrients, such as amino acids and glucose (*83*). In nutrient rich environments, TORC1 is active and phosphorylates downstream effectors to enhance anabolism and protein synthesis while repressing catabolism and autophagy. The opposite is true during starvation, which leads to inactivation of TORC1 and consequent upregulation of catabolism and autophagy (*78*).

Macroautophagy (hereafter autophagy) is a process where cytoplasmic biomolecules and organelles are engulfed in double-membraned compartments (autophagosomes) and are delivered to the vacuolar lumen. Cargo recruitment to autophagosomes may occur indiscriminately through bulk autophagy or may target specific organelles or molecules through selective autophagy (*84*). Bulk autophagy can be induced pharmacologically by rapamycin (*85*), a macrolide that forms a complex with Fpr1 (FKBP12 in humans) to directly inhibit TORC1 (*70, 73-75, 86*). Under these conditions, TORC1 directs the delivery of cytoplasmic contents to the vacuole for their degradation to resupply the cell with free metabolites, prolonging cell survival during nutritional stress (*84*). A core component of all autophagy pathways is the Atg8 proteins (ortholog of mammalian LC3) that decorate the autophagosome during its formation (*87*). Atg8 is a core autophagy protein involved in both bulk and selective autophagy pathways. It coordinates the expansion and maturation of the autophagosome in both pathways (*88*), while providing recruitment sites for specific cargo and selective autophagy receptors (SAR) in selective autophagy (*87*). Atg8 therefore is responsible for the creation of large autophagosomes (*89*) and mediates delivery of specific cargos to the vacuole.

TORC2 is localized at the cytoplasmic side of the PM (*90, 91*), where it primarily responds to membrane stress, osmotic stress, and sphingolipid deprivation (*92, 93*). TORC2 regulates actin polarization, sphingolipid biosynthesis, and endocytosis. Aside from its structural and functional differences, TORC2 is dissimilar to TORC1 in two ways: 1) stress upregulates the activity of the complex (*94-96*) and 2) it is insensitive to rapamycin (*76*). Stressors appear to increase the activity of TORC2, promoting sphingolipid synthesis and the cell wall integrity pathway through the AGC kinases Ypk1 (homolog of mammalian SGK1) (*96, 97*). Regulation of endocytosis through TORC2 activity is not unidirectional, as some studies have found that it upregulates endocytosis (*98, 99*) while others have found that it downregulates endocytosis (*100, 101*). TORC2 insensitivity to rapamycin is due to the masking of its FKBP12-Rapamycin Binding (FRB) domain on Tor2 by the TORC2 subunit Avo3 (*102*). Together TORC1 and TORC2 create different contexts for TOR signaling to regulate growth and metabolism in response to various stressors.

During the pheromone response, cytoplasmic proteins have been found to accumulate in the vacuole (*103*), a hallmark of autophagy despite the lack of nutritional stress. This led us to investigate potential interactions between TOR signaling and the mating pathway. Here, we show that TOR signaling mediates the surface presentation of all GPCRs in *S. cerevisiae* during starvation, specifically leading to the internalization of the mating receptors. Coincident with effects on localization, we find that TORC signaling dampens mating pathway output during starvation. Surprisingly, we find that the rapamycin-induced effect on mating receptor localization and pathway output is dependent upon the rapamycin-insensitive TORC2 signaling through its effector kinase Ypk1. Rapamycin effects on Ste2 are ligand-independent, but we also found that TORC1 and TORC2 signaling pathways impact ligand-dependent signaling. This includes suppression of pathway signaling by the central autophagy protein Atg8. Thus, yeast GPCRs are regulated by TOR in both ligand-dependent and ligand-independent contexts.

RESULTS

Nutrient availability regulates surface presentation of the mating GPCR Ste2.

Given, that the yeast mating response stops mitotic reproduction and involves a significant amount of new growth (*43-46*), we hypothesized that cells experiencing nutrient deprivation might alter mating signaling pathway to prevent mating while malnourished. The GPCR Ste2 initiates mating signaling and seemed to be a likely target for regulation. To test this, we examined cells expressing Ste2-mEnvy from a culture grown to saturation. Cells were grown to the stationary phase of growth (OD600 > ~1.2-1.5) to create a nutrient-deprived environment or maintained in the nutrient-rich mid-log phase of growth (OD600 < 0.8), and then imaged by fluorescence microscopy (Fig. 1A). Cells in the mid-log phase showed typical receptor localization patterns, Ste2 was present on the PM and inside the vacuole of the cell. However, cells grown to stationary phase showed a 62% reduction in abundance at the PM (Fig. 1B). We tested whether this was a reversible effect by diluting stationary phase cells and supplementing them with fresh nutrients over 4.5 hours. The control group was sustained in mid-log growth by regular media changes. Previously-starved cells showed a complete recovery of PM-associated Ste2 after 1.5 hours in replete media (Fig. 1B). This shows that the available nutrients determines the spatial localization of the mating receptor.

We would predict that the saturated culture media is depleted of a variety of nutrients, but we hypothesized that this might be specifically related to TOR signaling, which is regulated by nitrogen depletion (*83*). Cells were kept at a sub-saturating density (OD600 = 0.2-0.8) in standard Synthetic Complete (SC) media, and then diluted into low-nitrogen SC media for 6 hours. Cells were constantly maintained in the mid-log phase of growth throughout the experiment and imaged by fluorescence microscopy (Fig. 1C). Cells in nitrogen-limited media showed a 66% reduction of Ste2 abundance at the cell periphery while in the mid-log phase of growth (Fig. 1D). Thus, the localization of Ste2 to the PM is specifically sensitive to nitrogen levels in the media.

Ste2 plasma membrane levels and mating transcription is altered by TORC1.

Having found that nitrogen availability controls Ste2 levels on the PM, we hypothesize that the nitrogen-sensitive TORC1 may control the cell signaling that leads to changes in receptor localization. Rapamycin specifically represses TORC1 activity, mimicking the effects of nitrogen depletion (*70, 73-75*). We treated cells with 0.2μM rapamycin in SC media during mid-log growth for 2 hours, followed by imaging cells expressing Ste2-mEnvy using fluorescence microscopy. (Fig. 2A). Rapamycin treatment led to a 60% reduction in peripheral Ste2 levels (Fig. 2E), showing TORC1 signaling is responsible for starvation-induced internalization of the receptor.

There are three potential explanations for this effect: 1) PM proteins could be internalized indiscriminately, 2) this effect could be specific to Ste2, 3) or this effect could be selective to GPCRs. There are three GPCRs in yeast: the mating receptors Ste2 and Ste3, and the sugar receptor Gpr1 (*104*). We generated strains with each other two yeast GPCRs, Ste3 and Gpr1 tagged with mEnvy, and treated these cells with 0.2 μM rapamycin. When we observed their PM levels through fluorescence microscopy (Fig. 2B,C), rapamycin treatment changed the localization of both GPCRs. Ste3 levels at the PM decreased by 22%, while Gpr1 abundance increased by 40% (Fig. 2E). To test whether this effect is specific to GPCRs, we created a strain with the proton pump Pma1 (*105*) labeled with mRuby2 and performed the same rapamycin experiment as above (Fig. 2D,E). Pma1 localization to the PM showed a 16% increase in the presence of rapamycin (Fig 2E). These results show that TORC1 inhibition does not cause indiscriminate endocytosis of integral membrane proteins, as demonstrated by the increase in the abundance of both Gpr1 and Pma1 at the periphery. Further, while this alteration of surface presentation does not appear to be specific to GPCRs, inhibition of TORC1 alters the localization of every GPCR in yeast.

The reduced surface presentation of Ste2 during TORC1 inhibition led us to hypothesize that rapamycin-treated cells would have a diminished pheromone response. To test this, we measured pheromone-dependent transcription in the presence and absence of rapamycin using a pheromone-responsive β-galactosidase assay (Fig. 2F). We found that rapamycin treatment reduces the maximal transcriptional output (E_{max}) of mating genes by 26%. Rapamycin had no effect on the EC_{50}. This suggests that the endocytosis of Ste2 through TORC1 inhibition serves to repress the capacity of the cell to respond to mating pheromone.

TORC1-dependent endocytosis occurs through CME and TORC2 signaling.

In order to determine the components in the pathway linking TORC1 signaling to loss of Ste2 from the PM, we constructed fifteen strains with deletions of genes known to be involved in either TORC signaling, Ste2 endocytosis, and clathrin-mediated endocytosis (CME) (Fig. 3A). These cells were treated with 0.2µM rapamycin for 2 hours, and peripheral Ste2 levels were measured using fluorescence microscopy. Each deletion mutant was then grouped into one of three categories which denotes their effect on rescuing Ste2 abundance at the PM with rapamycin: 1) no rescue (Fig. S1), 2) partial rescue, and 3) complete rescue (Fig. 3B).

We found that deleting End3 partially blocks the effect of rapamycin on Ste2 localization on the PM (Fig. 3B,C). End3 is an adaptor protein that facilitates the internalization step in CME. Cells that lack End3 show defects in endocytosis and have been reported to reduce internalization of Ste2 by ~60-80% (*106, 107*). CME in these cells is defective, but not entirely absent. We also saw that deletion of Rod1 partially blocked the effect of rapamycin on Ste2 localization (Fig 3B,E). In contrast, deleting the α-arrestin Rog3 completely blocked rapamycin-induced internalization of Ste2 (Fig 3B,D). The α-arrestins Rod1 and Rog3 are paralogs that facilitate CME and desensitization of active Ste2 in response to pheromone (*25, 59*). The use of Rod1, Rog3, and End3 all indicate that TORC1 inhibition may lead to CME of Ste2 .

Rod1 and Rog3 are known to associate with the phosphorylated C-terminus of active Ste2 (*25, 59*), suggesting that C-terminal modification of Ste2 is required for this internalization event. To test this, we replaced the C-terminus of Ste2 with EGFP (*ste2^{T326}-EGFP*) in cells, and then treated with rapamycin as described above (Fig. 4A). Ste2^{T326} levels at the PM did not change when treated with rapamycin (Fig. 4B), confirming that the internalization of the receptor is reliant on C-terminal modifications, particularly phosphorylation.

Finally, we found that deleting Ypk1 completely blocks the effect of rapamycin on Ste2 PM levels (Fig 3B,F). Ypk1-mEnvy localizes to the tip of the mating projection (Fig. 5), consistent with a role in the regulation of receptor endocytosis. Ypk1 is thought to be activated by TORC2, but we wanted to rule out the possibility that TORC1 was activating Ypk1. We tested this by truncating Avo3 to create a rapamycin-sensitive TORC2 strain because Tor2 is essential. We generated an Avo3 truncation in cells harboring a labeled Ste2 (*avo3^{T1273} STE2-mENVY*). These cells were treated with rapamycin as described above, leading to the inhibition of both TORC1 and TORC2 (Fig. 6A). Rapamycin treatment did not reduce Ste2 levels at the PM (Fig. 6B), suggesting TORC2 activity is required for receptor internalization during TORC1 inhibition. These results confirm that Ste2 localization is being controlled by TORC2 signaling through Ypk1.

Pheromone-induced autophagy represses mating transcription through cytoplasmic clearance of Ste2.

Ligand binding to Ste2 drives its internalization and vacuolar targeting. Here, we have shown that TORC signaling drives endocytosis of Ste2 in the absence of ligand. We hypothesized that the pheromone response might take advantage of TORC signaling to negatively regulate mating signaling. We tested this by deleting the gene for the core autophagy protein Atg8 from cells expressing Ste2-mEnvy and treating with 10µM pheromone. We used the β-galactosidase assay described above to measure mating gene transcription in *atg8*Δ and wild-type cells (Fig. 7A). Cells lacking Atg8 showed a 30% increase in transcriptional output compared to wild-type cells,

without shifting the EC_{50}. Therefore, autophagy during the pheromone response contributes to the attenuation of pheromone-induced transcription.

Ypk1 suppresses mating transcription in response to pheromone.

We have found that Ypk1 is required for rapamycin-induced Ste2 endocytosis. We hypothesize that Ypk1 may be responsible for the concomitant reduction in mating transcription during the pheromone response. To test this, we performed a β-galactosidase assay as described above to measure transcriptional output of cells lacking Ypk1 (Fig. 7B). These cells show a remarkable 433% increase in transcription of mating genes and a 39% decrease in EC_{50}. This indicates that Ypk1 is a negative regulator of the pheromone pathway in the absence of rapamycin or nutritional stress.

DISCUSSION

Here we describe both ligand-dependent and ligand-independent regulation of the GPCR, Ste2, by TOR complexes and their effectors. We have shown that nutrient limitation leads to the differential levels on the PM for all GPCRs in *S. cerevisiae* through TORC1 signaling, decreasing levels of the mating receptors Ste2 and Ste3, while increasing levels of the hexose receptor, Gpr1. These changes in Ste2 localization were concomitant with decreased transcription downstream of Ste2. Through analysis of 15 different candidate genes by deletion analysis and additional truncations of Avo3 and the receptor itself, we determined that the signaling pathway from TORC1 inhibition to loss of Ste2 from the PM was dependent upon TORC2-Ypk1 signaling and α-arrestin recruitment to the receptor, followed by End3-dependent clathrin mediated endocytosis. These impacts on Ste2 lead us to examine the effect of TORC effectors on ligand-dependent transcription. We have shown that the central autophagy protein, Atg8, is involved in suppressing pheromone pathway output. We also show that the TORC2 effector Ypk1 downregulates the mating response.

Why suppress mating with TOR?

Cells may reduce their mating receptor levels in response to starvation to avoid mating while hungry. There is an increased risk of cell death while responding to pheromone (*49*). If cells are stressed due to a lack of carbon sources and metabolites, mating may exacerbate this stress by committing significant energy and resources toward forming a mating projection. In this situation, it would be advantageous to prevent the mating response. As the GPCRs at the beginning of the pathway, Ste2 and Ste3 are prime candidates for regulation. In this regard, the finding that both Ste2 and Ste3 are removed from the PM suggests that the cell uses TOR signaling pathways to suppress mating when nutrients are limiting. Consistent with this model of celibate hungry yeast, we found that the sole nutritional GPCR, Gpr1, accumulates on the PM in response to TOR inhibition. Increased surface presentation of Gpr1 would help ensure that the cell is prepared to deal with low nutrient environment through pseudohyphal growth (*108*).

Interestingly, we have observed that Ste3 has a less dramatic effect in response to rapamycin than Ste2. This may be because Ste2 is trafficked to the vacuole after internalization (*65, 66*), while Ste3 is recycled (*67*). It is possible that TORC1 inhibition stimulates Ste3 internalization, but a subset of internalized receptor is recycled back to the PM, leading to a diminished impact of TOR signaling. This is particularly interesting in that TORC inhibition during starvation is not

solely inducing a large-scale endocytic event across the PM. Rather, the result is a differential modulation in surface presentation of each yeast GPCR to adapt cellular responses to the needs of the cell in nutrient-deprived conditions.

TOR-dependent endocytosis vs Ligand-Induced Endocytosis

We have found that TORC1-induced endocytosis of Ste2 is a distinct process from receptor-mediated internalization. During the pheromone response, Ste2 internalization is mediated primarily by three sets of proteins that interact with the receptor C-terminus: 1) the yeast casein kinases Yck1 and Yck2 (*54-56*), 2) the α-arrestins Rog3 and Rod1 (*25, 59*), and 3) the epsin-like proteins Ent1 and Ent2 (*63, 64*). Starvation-induced endocytosis aligns with receptor mediated internalization in that 1) the receptor C-terminus is a required component, 2) it is mediated by α-arrestins, and 3) it is clathrin-mediated as shown by our deletion screen hits (End3, Rog3, and Rod1) and ste2^{T326} experiments. However, the preferential use of the arrestins in TORC1-mediated internalization makes TORC1-mediated internalization unique from receptor-mediated endocytosis. Prior studies have shown that a double deletion of *ROG1* and *ROG3* cause significant defects in receptor-mediated Ste2 endocytosis, whereas single deletions of these genes show no significant effect (*25*). This may suggest that these proteins are redundant in their function during mating. However, we find that Rog3 is preferentially used in TORC1-mediated internalization. While Rog3 may partially compensate for Ste2 internalization in the absence of Rod1, Rod1 does not seem to notably contribute to Ste2 endocytosis in the absence of Rog3. This may be due to differential phosphorylation patterns between starvation and mating. There are 33 serine and threonine residues in the C-terminal region of Ste2 that can be phosphorylated. Kim et al. found that specific residues contribute to different aspects of both receptor internalization and signaling during mating (*109*). Therefore, differential patterns of receptor phosphorylation may lead to preferential recruitment of endocytic adapter proteins, like Rog3, during starvation. Another key difference is that TORC1-mediated internalization does not seem to require Yck1 or Yck2. It is possible that this is due to the redundant functions of these kinases (*54*), with one Yck compensating for the lack of the other. However, another kinase, such as Ypk1, may be responsible for the direct phosphorylation of the receptor during starvation.

Activation of TORC2 by inhibition of TORC1

We have found an interesting crossroad in TORC signaling whereby TORC1 signaling appears to directly impact TORC2 activity. TORC1 and TORC2 are stress-responsive complexes that regulate cellular growth and metabolism. These complexes are structurally and functionally distinct. However, there are instances where TORC1 and TORC2 signaling pathways intertwine to tune the magnitude of their responses (*110, 111*). For example, while TORC1 is the primary regulator of autophagy during nitrogen starvation, TORC2 activity has been suggested to enhance autophagy specifically in the absence of amino acids (*110*). We have found that both TORC1 and TORC2 contribute to rapamycin-induced endocytosis of Ste2. This indicates that TORC1 and TORC2 signaling are connected in some way, the specific mechanism of which is yet to be characterized. This may represent a novel interaction between TORC1 and TORC2 where one regulates the signaling of the other directly at the complex level, but further investigation of this interaction and pathway are required.

We have further characterized the role of Ypk1 in internalization as a promoter of receptor endocytosis. Ypk1 is known to play a regulatory role in endocytosis through the TORC2 signaling pathway, but there are studies suggesting it either promotes or represses endocytosis

depending on the circumstance (*98-101*). Some studies suggest that Ypk1 activity promotes receptor endocytosis (*98*), while others suggest that Ypk1 downregulates Rod1 to repress Ste2 internalization (*100*). Our studies suggest that Ypk1 promotes Ste2 internalization, at a minimum during nutrient deprivation, and potentially during the pheromone response, where there is a marked effect on transcriptional output that may be due to the observed effects on receptor endocytosis. Our studies provide yet another context where Ypk1 regulates endocytosis, but more work on Ypk1 and endocytosis will need to be done to resolve these differences.

We found that TOR signaling impacted localization of every GPCR in yeast, in a ligand-independent manner. There are reports that β_2-Adrenergic Receptor is targeted to the lysosome in ligand-dependent manner in mammals (*112*). Together, these data suggest that TOR regulation of GPCRs may be broadly conserved. We do not know why yeast initiate autophagy during the pheromone response. One potential explanation is that it frees metabolites to support growth of the mating projection. However, our data is consistent with a different explanation. We have found that pheromone-induced autophagy dampens the mating pathway. Perhaps mating stimulates autophagic clearance of cytosolic proteins to remove active receptor from the cytosol. In mammalian cells, GPCR trafficking to various subcellular locations following internalization leads to unique signaling profiles (*39-42*). It is possible that Ste2 may likewise signal at the endosome. In this scenario, the cell would rely upon Atg8 and autophagy to suppress endosomal signaling by directing Ste2 to the vacuole.

There are limitations in our interpretations of our data which should be considered. Our screen of genetic deletions has characterized certain proteins as playing a role in TORC1-mediated endocytosis. However, due to the existence of various paralogs that have arisen from whole genome duplication (*80*), we cannot entirely rule out proteins that did not rescue in our screen from playing a role in this process. For instance, the fact that single deletions of casein kinases Yck1 and Yck2 or epsin-like proteins Ent1 and Ent2 do not rescue Ste2 internalization in our screen does not rule them out as potential candidates of the pathway (*54, 61*), but double deletions of these proteins are inviable (*61, 113*).

GPCRs and the regulation of their signaling is significant to human health and physiology, seeing as they are the most targeted molecule by FDA-approved therapeutics (*9*). Therefore, understanding signaling cascades that control their output is crucial to therapeutic development for diseases that may arise from dysregulated GPCR signaling, such as heart failure and certain cancers (*10-12*). These studies open the doors to avenues of research at the intersection of GPCR and TOR signaling.

MATERIALS AND METHODS

Yeast Strains

Strains reported in this study are listed in Table S1. All strains were constructed in the MAT**a** haploid *Saccharomyces cerevisiae* parent strain BY4741, except for those used to visualize Ste3. In which case, strains were constructed in the MATα haploid parent strain BY4742. Strains containing fluorescent labeled, deleted, or truncated genes were created through oligonucleotide-directed homologous recombination using primers listed in Table S2. Primer amplicons were generated through PCR using Q5 Hot Start High-Fidelity 2X Master Mix (NEB #M0494). G-protein-coupled receptors (Ste2, Ste3, Gpr1) and Ypk1were labeled with monomeric Envy

(mEnvy/Envy^{V206K}). EGFP sourced from pFA6a-link-yoEGFP-SpHis5 (Addgene Plasmid #44836) (*114*) was used to label and truncate Ste2 simultaneously. Pma1 labeling is discussed below. Genetic deletions and the Avo3 truncation were generated by replacing the target locus with a geneticin resistance cassette (KanMX6). This cassette was sourced from a Yeast Deletion Library (Dharmacon) or from the pFA6a-yo-linkEGFP-KanMX plasmid (Addgene Plasmid #44900) (*114*).

Cells were grown in Yeast Extract-Peptone-Dextrose (YPD) growth media at 30°C. PCR products were transformed into parent yeast strains using a standard lithium acetate transformation with single-stranded carrier DNA and PEG (). These cultures were grown on standard selective media (SCD his- or YPD G418+) and isolated via auxotrophic or geneticin resistance-based selection. Transformants were verified using PCR and fluorescence microscopy when applicable. PCR verification was performed using One*Taq* 2X Master Mix with Standard Buffer (NEB #M0482) or LongAmp Hot Start *Taq* 2X Master Mix (NEB #M0533).

Yeast Cell Culture for Microscopy

Cells were grown overnight in 0.22µm-filtered Synthetic Complete + Dextrose (SC) media at 30°C to an OD600 of 0.2-0.8. To limit cells of nitrogen sources, cell were diluted from SC media into low nitrogen SC media (SC ammonium sulfate-, uracil-, L-histidine-, L-leucine-) and incubated for 6 hours prior to imaging. To repress TORC1 activity with rapamycin, cells were treated with 0.2 µM rapamycin in ethanol for 2 hours prior to imaging. To induce the mating response, cells were treated with 10 µM α-factor in water for 2 hours prior to imaging. All cells were imaged on 2% agarose pads. Agarose pads were supplemented with equal concentration of rapamycin or pheromone where applicable.

Live-cell Widefield Microscopy

Live-cell microscopy experiments were conducted using an IX83 (Olympus) widefield microscope and a Prime 95B CMOS camera (Photometrics) operated through cellSens Dimension 1.18 (Olympus). All images were acquired using a UPlanXApo 100X Oil objective (Olympus). Fluorescence illumination was performed using an X-Cite 120 LEDBoost (Excelitas) at 40% light intensity. Reflected fluorescence exposure time was 3s to image Ste2/3 and Ypk1, 10s for Gpr1, and 700ms for FM4-64.

Mating Gene Transcription Assays

Assays were performed based on the Beta-galactosidase Reporter Gene Assay (Liquid Form) from the Dohlman Lab (*115*). Cells were transformed with the plasmid pRS423-P_{FUS1}-LacZ as previously described. Colonies were isolated by growth on standard selective media (SCD his-). Cultures were grown in SCD his- media at 30°C to an OD600 of 0.1-0.8. Cells were pelleted at 2500 rpm for 5 minutes and resuspended in SCD his- media to obtain an OD_{600} of 0.6-0.8. In a polystyrene 96-well plate, 90µL of cells were added to 12 wells per row, whereby each row of wells contained the aliquots of a different transformant culture. Then, 10µL of α-factor (GenScript) was added to each well, whereby each column of wells contained different concentrations of the mating pheromone: e.g. 0µM, 0.003µM, 0.01µM, 0.03µM, 0.1µM… 300µM. Cells were gently shaken and incubated at 30°C for 90min. Solutions of 1mM fluorescein di-β-galactopyranoside (Invitrogen #F1179) diluted in 25mM potassium phosphate buffer pH 7.2 and 5% Triton X-100 diluted in 250mM potassium phosphate buffer pH 7.2 were mixed in equal parts. After the initial incubation 20µL of this solution was added to each well,

cells were gently shaken, covered in aluminum foil, and incubated at 37°C for 90min. The reaction was quenched with 20µL of 1M sodium bicarbonate and read on a fluorescent plate reader (Synergy 2) at an excitation wavelength of 485/20 and emission wavelength of 528/20. Fluorescent intensity values were normalized to cell culture density and averages were fit to a Hill Equation using the Curve Fitting Toolbox 3.8 in MATLAB to determine the E_{max}, EC_{50}, and Hill slope of the generated dose response curve. Lower bounds of these values were set to zero and upper bounds remained infinite.

Analysis of Peripheral GPCR Abundance

Z-stacks of fluorescent and differential interference contrast (DIC) images were acquired as previously described. In FIJI, a single slice of the fluorescent and DIC images in the middle of the Z-stack were isolated and saved as 16-bit TIFF files to be used for mask generation and analysis. These images were merged and qualitatively assessed as quality control to ensure that the isolated fluorescent and DIC frame exist in the same focal plane. The saved DIC images were loaded into Cellpose 2.0 (*116*) for mask generation. In Cellpose 2.0, the cyto2 pretrained model was used to generate masks for individual cells in each image, with a user-defined cell diameter of 80 pixels, a flow threshold (flow_threshold) of 0, and a mask threshold (cellprob_threshold) of 1.5. Any masks which did not encompass the entire cell were fixed or removed. Any masks that overlayed debris, dead cells, or cells that were partially out of frame were removed. Masks were saved as PNG files.

Masks were loaded into MATLAB and eroded with a diamond structuring element (1-pixel radius) to ensure individual cell masks are not touching. Masks were converted into a logical mask where every value over 0 is considered 'True', and all connected components with fewer than 5000 pixels were removed. The logical mask was then converted back to a double. Taking the difference between this mask eroded with a diamond structuring element (7-pixel radius) and the "un-eroded" mask generates a new mask that tracks values along the periphery of all cells in an image together. Converting this to a count mask generates the working mask used to measure the fluorescent intensity along the cell edge in individual cells.

Single-slice fluorescent images were loaded into MATLAB. A Gaussian Blur was applied to the image with a standard deviation (sigma) of 50 and subtracted from the original image. The mean fluorescent intensity was calculated from this image within the parameters defined by the previously described working mask for each individual cell.

Statistics

To determine whether two sample groups are significantly different, a Two-sample *t*-test was performed. Any p-value produced that was less than 0.05 deemed the two groups to have a difference in means that is statistically significant. This was performed for microscopy experiments in Fig. 1 and Fig. 2. When analyzing data curated from experiments using genetic mutants treated with rapamycin (Fig. 3, Fig. 4, and Fig. 6), a One-Way ANOVA was used. Four groups were analyzed in the ANOVA per experiment: the wild-type untreated cells, wild-type cell treated with rapamycin, mutant untreated cells, and mutants treated with rapamycin. ANOVA results were then processed through a multiple comparison test (Tukey's honest significance test). As described above, a p-value equal to or less than 0.05 denoted a significant difference between sample groups.

Mutagenesis of GFP Envy in an Epitope-Tagging Plasmid

The pFA6a-link-GFPEnvy-SpHis5 epitope tagging plasmid (Addgene Plasmid #60782) (*117*) was mutagenized such that the expressed Envy protein was incapable of dimerization. Val206 of Envy was mutagenized to Lys with the Q5 Site-Directed Mutagenesis Kit (NEB #E0554S) using primers listed in Table S2. The mutated product was transformed into chemically competent *Escherichia coli* (C2987H) through a High Efficiency Transformation (NEB). Colonies were isolated via growth on selective media (LB carbenicillin+). Colonies were grown in liquid selective media, and plasmids were purified using a Monarch Plasmid Miniprep Kit (NEB #T1010). Successful mutagenesis was verified through DNA sequencing (Plasmidsaurus).

Cloning pRSII405-*PMA1-mRUBY2*

A plasmid construct containing *PMA1-mRUBY2* was generated in a pRSII405 vector via Gibson Assembly. The sequence for *PMA1* was amplified from BY4741 genomic DNA, and the *mRUBY2* sequence was amplified from pFA6a-link-yomRuby2-Kan (Addgene Plasmid #44953) (*114*). Both amplicons were generated through PCR with Q5 Hot Start High-Fidelity 2X Master Mix (NEB #M0494) using primers listed in Table S2. The vector, pRSII415 (Addgene Plasmid #35440) (*118*) was digested by SacII (NEB #R1057) and HindIII-HF (NEB #R3104). The cut vector was verified via band separation using gel electrophoresis, and the vector was extracted from the gel using a Monarch DNA Gel Extraction Kit (NEB #T1020). Gibson Assembly of the three generated fragments was performed using NEBuilder HiFi DNA Assembly Master Mix (NEB #E2621). The resulting assembly mixture was transformed into chemically competent *Escherichia coli* (C2987H) through a High Efficiency Transformation (NEB). Colonies were isolated via growth on selective media (LB carbenicillin+). Colonies were grown in liquid selective media, and plasmids were purified using a Monarch Plasmid Miniprep Kit (NEB #T1010). Constructs were then verified by restriction digest using SacI-HF (NEB #R3156) and SalI-HF (NEB #R3138) and through DNA sequencing (Plasmidsaurus). Verified plasmids were digested BamHI-HF (NEB #R3136) and transformed into yeast using the transformation methods described above. Colonies were grown on standard selective media (SCD leu-) and isolated via auxotrophic selection. Transformants were verified using PCR and fluorescence microscopy. PCR verification was performed using One*Taq* 2X Master Mix with Standard Buffer (NEB #M0482).

Supplementary Materials

Fig. S1. Single genetic deletions that do not block rapamycin-induced endocytosis.
Table S1. Yeast Strains.
Table S2. Primer List.

References and Notes:

1. D. M. Rosenbaum, S. G. Rasmussen, B. K. Kobilka, The structure and function of G-protein-coupled receptors. *Nature* **459**, 356-363 (2009).
2. M. C. Lagerstrom, H. B. Schioth, Structural diversity of G protein-coupled receptors and significance for drug discovery. *Nat Rev Drug Discov* **7**, 339-357 (2008).
3. W. M. Oldham, H. E. Hamm, How do receptors activate G proteins? *Adv Protein Chem* **74**, 67-93 (2007).

4. J. J. Dumas, D. G. Lambright, Gs alpha meets its target--shedding light on a key signal transduction event. *Structure* **6**, 407-411 (1998).
5. P. A. Oude Weernink, L. Han, K. H. Jakobs, M. Schmidt, Dynamic phospholipid signaling by G protein-coupled receptors. *Biochim Biophys Acta* **1768**, 888-900 (2007).
6. N. C. Law, M. F. White, M. E. Hunzicker-Dunn, G protein-coupled receptors (GPCRs) That Signal via Protein Kinase A (PKA) Cross-talk at Insulin Receptor Substrate 1 (IRS1) to Activate the phosphatidylinositol 3-kinase (PI3K)/AKT Pathway. *J Biol Chem* **291**, 27160-27169 (2016).
7. M. M. Belcheva, C. J. Coscia, Diversity of G protein-coupled receptor signaling pathways to ERK/MAP kinase. *Neurosignals* **11**, 34-44 (2002).
8. H. Jiang, D. Galtes, J. Wang, H. A. Rockman, G protein-coupled receptor signaling: transducers and effectors. *Am J Physiol Cell Physiol* **323**, C731-C748 (2022).
9. A. S. Hauser, M. M. Attwood, M. Rask-Andersen, H. B. Schioth, D. E. Gloriam, Trends in GPCR drug discovery: new agents, targets and indications. *Nat Rev Drug Discov* **16**, 829-842 (2017).
10. H. A. Rockman, W. J. Koch, R. J. Lefkowitz, Seven-transmembrane-spanning receptors and heart function. *Nature* **415**, 206-212 (2002).
11. M. J. Marinissen, J. S. Gutkind, G-protein-coupled receptors and signaling networks: emerging paradigms. *Trends Pharmacol Sci* **22**, 368-376 (2001).
12. S. Rajagopal, S. K. Shenoy, GPCR desensitization: Acute and prolonged phases. *Cell Signal* **41**, 9-16 (2018).
13. P. Tsao, T. Cao, M. von Zastrow, Role of endocytosis in mediating downregulation of G-protein-coupled receptors. *Trends Pharmacol Sci* **22**, 91-96 (2001).
14. S. S. Ferguson, Evolving concepts in G protein-coupled receptor endocytosis: the role in receptor desensitization and signaling. *Pharmacol Rev* **53**, 1-24 (2001).
15. H. G. Dohlman, D. Apaniesk, Y. Chen, J. Song, D. Nusskern, Inhibition of G-protein signaling by dominant gain-of-function mutations in Sst2p, a pheromone desensitization factor in Saccharomyces cerevisiae. *Mol Cell Biol* **15**, 3635-3643 (1995).
16. J. B. O'Brien, J. C. Wilkinson, D. L. Roman, Regulator of G-protein signaling (RGS) proteins as drug targets: Progress and future potentials. *J Biol Chem* **294**, 18571-18585 (2019).
17. Y. Kim, S. Ghil, Regulators of G-protein signaling, RGS2 and RGS4, inhibit protease-activated receptor 4-mediated signaling by forming a complex with the receptor and Galpha in live cells. *Cell Commun Signal* **18**, 86 (2020).
18. N. Watson, M. E. Linder, K. M. Druey, J. H. Kehrl, K. J. Blumer, RGS family members: GTPase-activating proteins for heterotrimeric G-protein alpha-subunits. *Nature* **383**, 172-175 (1996).
19. W. I. Weis, B. K. Kobilka, The Molecular Basis of G Protein-Coupled Receptor Activation. *Annu Rev Biochem* **87**, 897-919 (2018).
20. D. M. Berman, T. Kozasa, A. G. Gilman, The GTPase-activating protein RGS4 stabilizes the transition state for nucleotide hydrolysis. *J Biol Chem* **271**, 27209-27212 (1996).
21. E. M. Ross, T. M. Wilkie, GTPase-activating proteins for heterotrimeric G proteins: regulators of G protein signaling (RGS) and RGS-like proteins. *Annu Rev Biochem* **69**, 795-827 (2000).

22. S. P. Srinivasa, N. Watson, M. C. Overton, K. J. Blumer, Mechanism of RGS4, a GTPase-activating protein for G protein alpha subunits. *J Biol Chem* **273**, 1529-1533 (1998).
23. M. R. Koelle, H. R. Horvitz, EGL-10 regulates G protein signaling in the C. elegans nervous system and shares a conserved domain with many mammalian proteins. *Cell* **84**, 115-125 (1996).
24. D. M. Apanovitch, K. C. Slep, P. B. Sigler, H. G. Dohlman, Sst2 is a GTPase-activating protein for Gpa1: purification and characterization of a cognate RGS-Galpha protein pair in yeast. *Biochemistry* **37**, 4815-4822 (1998).
25. C. G. Alvaro *et al.*, Specific α-arrestins negatively regulate Saccharomyces cerevisiae pheromone response by down-modulating the G-protein-coupled receptor Ste2. *Mol Cell Biol* **34**, 2660-2681 (2014).
26. A. Patwardhan, N. Cheng, J. Trejo, Post-Translational Modifications of G Protein-Coupled Receptors Control Cellular Signaling Dynamics in Space and Time. *Pharmacol Rev* **73**, 120-151 (2021).
27. J. A. Pitcher, N. J. Freedman, R. J. Lefkowitz, G protein-coupled receptor kinases. *Annu Rev Biochem* **67**, 653-692 (1998).
28. J. G. Krupnick, V. V. Gurevich, J. L. Benovic, Mechanism of quenching of phototransduction. Binding competition between arrestin and transducin for phosphorhodopsin. *J Biol Chem* **272**, 18125-18131 (1997).
29. U. Wilden, Duration and amplitude of the light-induced cGMP hydrolysis in vertebrate photoreceptors are regulated by multiple phosphorylation of rhodopsin and by arrestin binding. *Biochemistry* **34**, 1446-1454 (1995).
30. X. Tian, D. S. Kang, J. L. Benovic, beta-arrestins and G protein-coupled receptor trafficking. *Handb Exp Pharmacol* **219**, 173-186 (2014).
31. D. R. Sibley, R. H. Strasser, J. L. Benovic, K. Daniel, R. J. Lefkowitz, Phosphorylation/dephosphorylation of the beta-adrenergic receptor regulates its functional coupling to adenylate cyclase and subcellular distribution. *Proc Natl Acad Sci U S A* **83**, 9408-9412 (1986).
32. H. Attramadal *et al.*, Beta-arrestin2, a novel member of the arrestin/beta-arrestin gene family. *J Biol Chem* **267**, 17882-17890 (1992).
33. M. J. Lohse, J. L. Benovic, J. Codina, M. G. Caron, R. J. Lefkowitz, beta-Arrestin: a protein that regulates beta-adrenergic receptor function. *Science* **248**, 1547-1550 (1990).
34. M. T. Drake, S. K. Shenoy, R. J. Lefkowitz, Trafficking of G protein-coupled receptors. *Circ Res* **99**, 570-582 (2006).
35. M. Bunemann, M. M. Hosey, G-protein coupled receptor kinases as modulators of G-protein signalling. *J Physiol* **517 (Pt 1)**, 5-23 (1999).
36. M. L. Mohan, N. T. Vasudevan, M. K. Gupta, E. E. Martelli, S. V. Naga Prasad, G-protein coupled receptor resensitization-appreciating the balancing act of receptor function. *Curr Mol Pharmacol*, (2012).
37. S. K. Shenoy, P. H. McDonald, T. A. Kohout, R. J. Lefkowitz, Regulation of receptor fate by ubiquitination of activated beta 2-adrenergic receptor and beta-arrestin. *Science* **294**, 1307-1313 (2001).
38. A. Marchese, J. L. Benovic, Agonist-promoted ubiquitination of the G protein-coupled receptor CXCR4 mediates lysosomal sorting. *J Biol Chem* **276**, 45509-45512 (2001).

39. D. S. Eiger, C. Hicks, J. Gardner, U. Pham, S. Rajagopal, Location bias: A "Hidden Variable" in GPCR pharmacology. *Bioessays* **45**, e2300123 (2023).
40. F. Liccardo, A. Luini, R. Di Martino, Endomembrane-Based Signaling by GPCRs and G-Proteins. *Cells* **11**, (2022).
41. N. G. Tsvetanova, R. Irannejad, M. von Zastrow, G protein-coupled receptor (GPCR) signaling via heterotrimeric G proteins from endosomes. *J Biol Chem* **290**, 6689-6696 (2015).
42. B. Plouffe, A. R. B. Thomsen, R. Irannejad, Emerging Role of Compartmentalized G Protein-Coupled Receptor Signaling in the Cardiovascular Field. *ACS Pharmacol Transl Sci* **3**, 221-236 (2020).
43. L. Bardwell, A walk-through of the yeast mating pheromone response pathway. *Peptides* **26**, 339-350 (2005).
44. Y. Wang, H. G. Dohlman, Pheromone signaling mechanisms in yeast: a prototypical sex machine. *Science* **306**, 1508-1509 (2004).
45. L. Merlini, O. Dudin, S. G. Martin, Mate and fuse: how yeast cells do it. *Open Biol* **3**, 130008 (2013).
46. A. C. Burkholder, L. H. Hartwell, The yeast alpha-factor receptor: structural properties deduced from the sequence of the STE2 gene. *Nucleic Acids Res* **13**, 8463-8475 (1985).
47. D. C. Hagen, G. McCaffrey, G. F. Sprague, Jr., Evidence the yeast STE3 gene encodes a receptor for the peptide pheromone a factor: gene sequence and implications for the structure of the presumed receptor. *Proc Natl Acad Sci U S A* **83**, 1418-1422 (1986).
48. C. G. Robertson, M. R. Clark-Cotton, D. J. Lew, Mechanisms that ensure monogamous mating in Saccharomyces cerevisiae. *Mol Biol Cell* **32**, 638-644 (2021).
49. N. N. Zhang, D. D. Dudgeon, S. Paliwal, A. Levchenko, E. Grote, K. W. Cunningham, Multiple signaling pathways regulate yeast cell death during the response to mating pheromones. *Mol Biol Cell* **17**, 3409-3422 (2006).
50. H. G. Dohlman, J. Song, D. Ma, W. E. Courchesne, J. Thorner, Sst2, a negative regulator of pheromone signaling in the yeast Saccharomyces cerevisiae: expression, localization, and genetic interaction and physical association with Gpa1 (the G-protein alpha subunit). *Mol Cell Biol* **16**, 5194-5209 (1996).
51. H. G. Dohlman, D. Apaniesk, Y. Chen, J. Song, D. Nusskern, Inhibition of G-Protein Signaling by Dominant Gain-of-Function Mutations in Sst2p, a Pheromone Desensitization Factor in Saccharomyces cerevisiae. *Molecular and Cellular Biology* **15**, 3635-3643 (1995).
52. T. R. Manney, Expression of the BAR1 gene in Saccharomyces cerevisiae: induction by the alpha mating pheromone of an activity associated with a secreted protein. *J Bacteriol* **155**, 291-301 (1983).
53. A. Banderas, M. Koltai, A. Anders, V. Sourjik, Sensory input attenuation allows predictive sexual response in yeast. *Nature Communications* **7**, 12590 (2016).
54. Y. Feng, N. G. Davis, Akr1p and the type I casein kinases act prior to the ubiquitination step of yeast endocytosis: Akr1p is required for kinase localization to the plasma membrane. *Mol Cell Biol* **20**, 5350-5359 (2000).
55. D. R. Ballon, P. L. Flanary, D. P. Gladue, J. B. Konopka, H. G. Dohlman, J. Thorner, DEP-domain-mediated regulation of GPCR signaling responses. *Cell* **126**, 1079-1093 (2006).

56. L. Hicke, B. Zanolari, H. Riezman, Cytoplasmic tail phosphorylation of the alpha-factor receptor is required for its ubiquitination and internalization. *J Cell Biol* **141**, 349-358 (1998).
57. J. Inglese, N. J. Freedman, W. J. Koch, R. J. Lefkowitz, Structure and mechanism of the G protein-coupled receptor kinases. *J Biol Chem* **268**, 23735-23738 (1993).
58. V. V. Gurevich, E. V. Gurevich, GPCR Signaling Regulation: The Role of GRKs and Arrestins. *Front Pharmacol* **10**, 125 (2019).
59. D. C. Prosser, A. E. Pannunzio, J. L. Brodsky, J. Thorner, B. Wendland, A. F. O'Donnell, α-Arrestins participate in cargo selection for both clathrin-independent and clathrin-mediated endocytosis. *J Cell Sci* **128**, 4220-4234 (2015).
60. A. F. Roth, N. G. Davis, Ubiquitination of the yeast a-factor receptor. *J Cell Biol* **134**, 661-674 (1996).
61. B. Wendland, K. E. Steece, S. D. Emr, Yeast epsins contain an essential N-terminal ENTH domain, bind clathrin and are required for endocytosis. *EMBO J* **18**, 4383-4393 (1999).
62. R. C. Aguilar, H. A. Watson, B. Wendland, The yeast Epsin Ent1 is recruited to membranes through multiple independent interactions. *J Biol Chem* **278**, 10737-10743 (2003).
63. S. C. Shih, D. J. Katzmann, J. D. Schnell, M. Sutanto, S. D. Emr, L. Hicke, Epsins and Vps27p/Hrs contain ubiquitin-binding domains that function in receptor endocytosis. *Nat Cell Biol* **4**, 389-393 (2002).
64. M. R. Dores, J. D. Schnell, L. Maldonado-Baez, B. Wendland, L. Hicke, The function of yeast epsin and Ede1 ubiquitin-binding domains during receptor internalization. *Traffic* **11**, 151-160 (2010).
65. P. K. Tan, N. G. Davis, G. F. Sprague, G. S. Payne, Clathrin facilitates the internalization of seven transmembrane segment receptors for mating pheromones in yeast. *J Cell Biol* **123**, 1707-1716 (1993).
66. K. A. Schandel, D. D. Jenness, Direct evidence for ligand-induced internalization of the yeast alpha-factor pheromone receptor. *Mol Cell Biol* **14**, 7245-7255 (1994).
67. L. Chen, N. G. Davis, Recycling of the yeast a-factor receptor. *J Cell Biol* **151**, 731-738 (2000).
68. D. C. Prosser, A. E. Pannunzio, J. L. Brodsky, J. Thorner, B. Wendland, A. F. O'Donnell, alpha-Arrestins participate in cargo selection for both clathrin-independent and clathrin-mediated endocytosis. *J Cell Sci* **128**, 4220-4234 (2015).
69. C. De Virgilio, R. Loewith, The TOR signalling network from yeast to man. *Int J Biochem Cell Biol* **38**, 1476-1481 (2006).
70. J. Heitman, N. R. Movva, M. N. Hall, Targets for cell cycle arrest by the immunosuppressant rapamycin in yeast. *Science* **253**, 905-909 (1991).
71. J. Kunz, R. Henriquez, U. Schneider, M. Deuter-Reinhard, N. R. Movva, M. N. Hall, Target of rapamycin in yeast, TOR2, is an essential phosphatidylinositol kinase homolog required for G1 progression. *Cell* **73**, 585-596 (1993).
72. E. J. Brown *et al.*, A mammalian protein targeted by G1-arresting rapamycin-receptor complex. *Nature* **369**, 756-758 (1994).
73. M. I. Chiu, H. Katz, V. Berlin, RAPT1, a mammalian homolog of yeast Tor, interacts with the FKBP12/rapamycin complex. *Proc Natl Acad Sci U S A* **91**, 12574-12578 (1994).

74. D. M. Sabatini, H. Erdjument-Bromage, M. Lui, P. Tempst, S. H. Snyder, RAFT1: a mammalian protein that binds to FKBP12 in a rapamycin-dependent fashion and is homologous to yeast TORs. *Cell* **78**, 35-43 (1994).
75. C. J. Sabers *et al.*, Isolation of a protein target of the FKBP12-rapamycin complex in mammalian cells. *J Biol Chem* **270**, 815-822 (1995).
76. R. Loewith *et al.*, Two TOR complexes, only one of which is rapamycin sensitive, have distinct roles in cell growth control. *Mol Cell* **10**, 457-468 (2002).
77. C. T. Keith, S. L. Schreiber, PIK-related kinases: DNA repair, recombination, and cell cycle checkpoints. *Science* **270**, 50-51 (1995).
78. R. Loewith, M. N. Hall, Target of rapamycin (TOR) in nutrient signaling and growth control. *Genetics* **189**, 1177-1201 (2011).
79. S. Wullschleger, R. Loewith, M. N. Hall, TOR signaling in growth and metabolism. *Cell* **124**, 471-484 (2006).
80. K. H. Wolfe, D. C. Shields, Molecular evidence for an ancient duplication of the entire yeast genome. *Nature* **387**, 708-713 (1997).
81. K. P. Wedaman, A. Reinke, S. Anderson, J. Yates, 3rd, J. M. McCaffery, T. Powers, Tor kinases are in distinct membrane-associated protein complexes in Saccharomyces cerevisiae. *Mol Biol Cell* **14**, 1204-1220 (2003).
82. S. Kira, Y. Kumano, H. Ukai, E. Takeda, A. Matsuura, T. Noda, Dynamic relocation of the TORC1-Gtr1/2-Ego1/2/3 complex is regulated by Gtr1 and Gtr2. *Mol Biol Cell* **27**, 382-396 (2016).
83. Y. Wang, X. Zheng, G. Li, X. Wang, TORC1 Signaling in Fungi: From Yeasts to Filamentous Fungi. *Microorganisms* **11**, (2023).
84. F. Reggiori, D. J. Klionsky, Autophagic processes in yeast: mechanism, machinery and regulation. *Genetics* **194**, 341-361 (2013).
85. T. Noda, Y. Ohsumi, Tor, a phosphatidylinositol kinase homologue, controls autophagy in yeast. *J Biol Chem* **273**, 3963-3966 (1998).
86. J. Heitman, N. R. Movva, M. N. Hall, Targets for Cell Cycle Arrest by the Immunosuppressant Rapamycin in Yeast. *Science* **253**, 905-909 (1991).
87. Y. K. Lee, J. A. Lee, Role of the mammalian ATG8/LC3 family in autophagy: differential and compensatory roles in the spatiotemporal regulation of autophagy. *BMB Rep* **49**, 424-430 (2016).
88. H. Nakatogawa, Y. Ichimura, Y. Ohsumi, Atg8, a ubiquitin-like protein required for autophagosome formation, mediates membrane tethering and hemifusion. *Cell* **130**, 165-178 (2007).
89. H. Abeliovich, W. A. Dunn, Jr., J. Kim, D. J. Klionsky, Dissection of autophagosome biogenesis into distinct nucleation and expansion steps. *J Cell Biol* **151**, 1025-1034 (2000).
90. J. Kunz, U. Schneider, I. Howald, A. Schmidt, M. N. Hall, HEAT repeats mediate plasma membrane localization of Tor2p in yeast. *J Biol Chem* **275**, 37011-37020 (2000).
91. T. W. Sturgill, A. Cohen, M. Diefenbacher, M. Trautwein, D. E. Martin, M. N. Hall, TOR1 and TOR2 have distinct locations in live cells. *Eukaryot Cell* **7**, 1819-1830 (2008).
92. J. Thorner, TOR complex 2 is a master regulator of plasma membrane homeostasis. *Biochem J* **479**, 1917-1940 (2022).
93. D. Rispal *et al.*, Target of Rapamycin Complex 2 Regulates Actin Polarization and Endocytosis via Multiple Pathways. *J Biol Chem* **290**, 14963-14978 (2015).

94. Y. Kamada *et al.*, Tor2 directly phosphorylates the AGC kinase Ypk2 to regulate actin polarization. *Mol Cell Biol* **25**, 7239-7248 (2005).
95. B. J. Niles, H. Mogri, A. Hill, A. Vlahakis, T. Powers, Plasma membrane recruitment and activation of the AGC kinase Ypk1 is mediated by target of rapamycin complex 2 (TORC2) and its effector proteins Slm1 and Slm2. *Proc Natl Acad Sci U S A* **109**, 1536-1541 (2012).
96. F. M. Roelants, D. K. Breslow, A. Muir, J. S. Weissman, J. Thorner, Protein kinase Ypk1 phosphorylates regulatory proteins Orm1 and Orm2 to control sphingolipid homeostasis in Saccharomyces cerevisiae. *Proc Natl Acad Sci U S A* **108**, 19222-19227 (2011).
97. D. E. Levin, Cell wall integrity signaling in Saccharomyces cerevisiae. *Microbiol Mol Biol Rev* **69**, 262-291 (2005).
98. A. K. deHart, J. D. Schnell, D. A. Allen, L. Hicke, The conserved Pkh-Ypk kinase cascade is required for endocytosis in yeast. *J Cell Biol* **156**, 241-248 (2002).
99. M. Riggi, C. Bourgoint, M. Macchione, S. Matile, R. Loewith, A. Roux, TORC2 controls endocytosis through plasma membrane tension. *J Cell Biol* **218**, 2265-2276 (2019).
100. C. G. Alvaro, A. Aindow, J. Thorner, Differential Phosphorylation Provides a Switch to Control How alpha-Arrestin Rod1 Down-regulates Mating Pheromone Response in Saccharomyces cerevisiae. *Genetics* **203**, 299-317 (2016).
101. F. M. Roelants *et al.*, TOR Complex 2-Regulated Protein Kinase Fpk1 Stimulates Endocytosis via Inhibition of Ark1/Prk1-Related Protein Kinase Akl1 in Saccharomyces cerevisiae. *Molecular and Cellular Biology* **37**, e00627-00616 (2017).
102. C. Gaubitz *et al.*, Molecular Basis of the Rapamycin Insensitivity of Target Of Rapamycin Complex 2. *Mol Cell* **58**, 977-988 (2015).
103. N. Rangarajan *et al.*, Systematic analysis of F-box proteins reveals a new branch of the yeast mating pathway. *J Biol Chem* **294**, 14717-14731 (2019).
104. M. Versele, K. Lemaire, J. M. Thevelein, Sex and sugar in yeast: two distinct GPCR systems. *EMBO Rep* **2**, 574-579 (2001).
105. R. Serrano, Characterization of the plasma membrane ATPase of Saccharomyces cerevisiae. *Molecular and Cellular Biochemistry* **22**, 51-63 (1978).
106. H. Benedetti, S. Raths, F. Crausaz, H. Riezman, The END3 gene encodes a protein that is required for the internalization step of endocytosis and for actin cytoskeleton organization in yeast. *Mol Biol Cell* **5**, 1023-1037 (1994).
107. S. Raths, J. Rohrer, F. Crausaz, H. Riezman, end3 and end4: two mutants defective in receptor-mediated and fluid-phase endocytosis in Saccharomyces cerevisiae. *J Cell Biol* **120**, 55-65 (1993).
108. H. Tamaki *et al.*, GPR1 regulates filamentous growth through FLO11 in yeast Saccharomyces cerevisiae. *Biochem Biophys Res Commun* **267**, 164-168 (2000).
109. K. M. Kim *et al.*, Multiple regulatory roles of the carboxy terminus of Ste2p a yeast GPCR. *Pharmacol Res* **65**, 31-40 (2012).
110. A. Vlahakis, M. Graef, J. Nunnari, T. Powers, TOR complex 2-Ypk1 signaling is an essential positive regulator of the general amino acid control response and autophagy. *Proc Natl Acad Sci U S A* **111**, 10586-10591 (2014).
111. S. Yerlikaya *et al.*, TORC1 and TORC2 work together to regulate ribosomal protein S6 phosphorylation in Saccharomyces cerevisiae. *Mol Biol Cell* **27**, 397-409 (2016).
112. R. P. Kommaddi, P. Y. Jean-Charles, S. K. Shenoy, Phosphorylation of the deubiquitinase USP20 by protein kinase A regulates post-endocytic trafficking of beta2

adrenergic receptors to autophagosomes during physiological stress. *J Biol Chem* **290**, 8888-8903 (2015).
113. L. C. Robinson, M. M. Menold, S. Garrett, M. R. Culbertson, Casein kinase I-like protein kinases encoded by YCK1 and YCK2 are required for yeast morphogenesis. *Mol Cell Biol* **13**, 2870-2881 (1993).
114. S. Lee, W. A. Lim, K. S. Thorn, Improved blue, green, and red fluorescent protein tagging vectors for S. cerevisiae. *PLoS One* **8**, e67902 (2013).
115. G. A. Hoffman, T. R. Garrison, H. G. Dohlman, Analysis of RGS proteins in Saccharomyces cerevisiae. *Methods Enzymol* **344**, 617-631 (2002).
116. M. Pachitariu, C. Stringer, Cellpose 2.0: how to train your own model. *Nat Methods* **19**, 1634-1641 (2022).
117. C. J. Slubowski, A. D. Funk, J. M. Roesner, S. M. Paulissen, L. S. Huang, Plasmids for C-terminal tagging in Saccharomyces cerevisiae that contain improved GFP proteins, Envy and Ivy. *Yeast* **32**, 379-387 (2015).
118. M. K. Chee, S. B. Haase, New and Redesigned pRS Plasmid Shuttle Vectors for Genetic Manipulation of Saccharomycescerevisiae. *G3 (Bethesda)* **2**, 515-526 (2012).
119. H. E. Manenschijn, A. Picco, M. Mund, A. S. Rivier-Cordey, J. Ries, M. Kaksonen, Type-I myosins promote actin polymerization to drive membrane bending in endocytosis. *Elife* **8**, (2019).
120. M. Moreno-Torres, M. Jaquenoud, C. De Virgilio, TORC1 controls G1-S cell cycle transition in yeast via Mpk1 and the greatwall kinase pathway. *Nat Commun* **6**, 8256 (2015).
121. A. Muir, S. Ramachandran, F. M. Roelants, G. Timmons, J. Thorner, TORC2-dependent protein kinase Ypk1 phosphorylates ceramide synthase to stimulate synthesis of complex sphingolipids. *Elife* **3**, (2014).

Acknowledgments:

The authors wish to thank past and current Kelley Lab Members for logistical and experimental input.

Funding:

National Institutes of Health grant P20GM144265 (JBK)
National Institutes of Health grant R15GM140409 (JBK)
Frederick Radke Undergraduate Research Fellowship, University of Maine (TD)

Author contributions:

Conceptualization: NRL, JBK
Data Curation: NRL
Formal Analysis: NRL
Funding Acquisition: JBK, TD
Investigation: NRL, TD, SS, CJ
Methodology: NRL, JBK
Project Administration: NRL, JBK

Resources: JBK
Software: NRL, JBK
Supervision: JBK
Validation: NRL, JBK
Visualization: NRL, JBK
Writing – Original Draft: NRL, JBK
Writing – Review & Editing: NRL, JBK

Competing interests:

Authors declare that they have no competing interests.

Data and materials availability:

MATLAB scripts used for the analysis of receptor localization at the plasma membrane are available on GitHub (https://github.com/Kelley-Lab-Computational-Biology). All data are available in the main text or the supplementary materials.

Figure Legends:

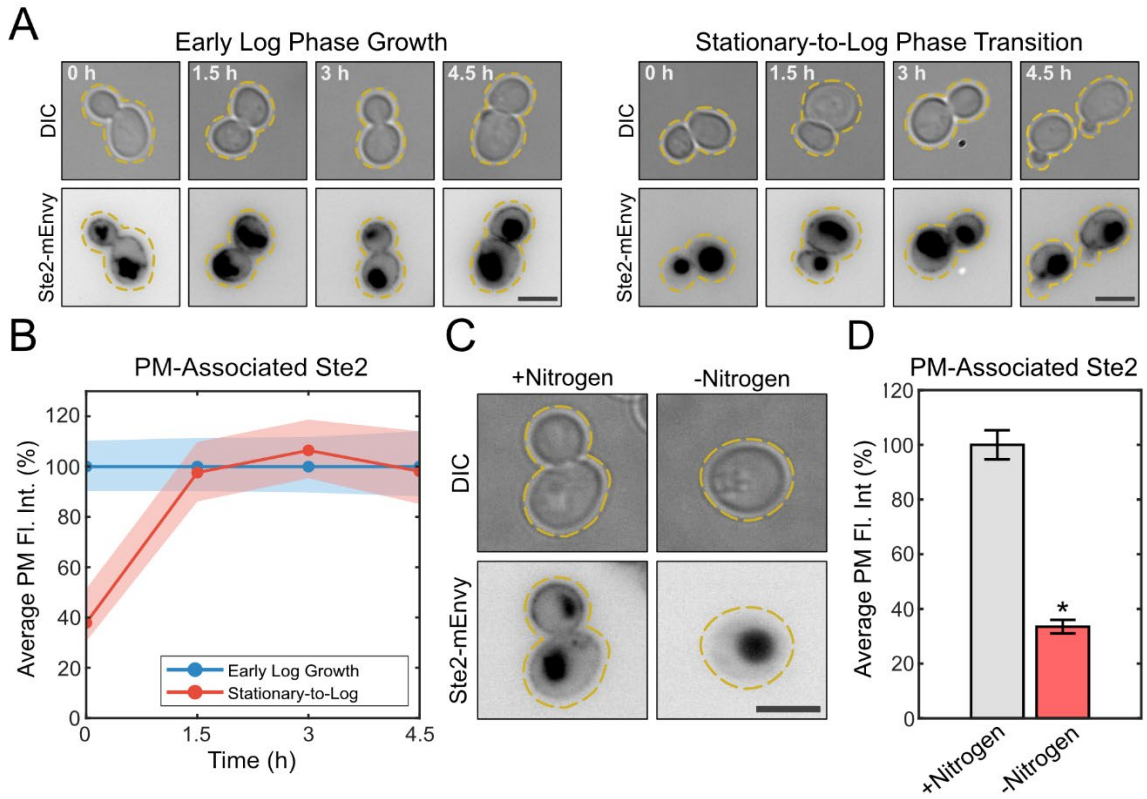

Fig. 1. Nutrient availability regulates Ste2 levels at the PM. (**A**) Representative images of cells expressing Ste2-mEnvy maintained in the log phase of growth (left panels) or grown to stationary phase and then diluted in replete media (right panels) for 4.5h. Scale bars represent 4µm. (**B**) Quantification of Ste2-mEnvy mean fluorescent intensity at the plasma membrane every 1.5h either during early log phase growth or growth from stationary phase into replete media (n > 130 cells). Measurements were normalized to the mean of "Early Log Growth" values at each timepoint to produce percentages. Shaded areas represent 95% bootstrap confidence intervals. (**C**) Representative images of cells expressing Ste2-mEnvy grown in SC media (+Nitrogen) or low nitrogen SC media (-Nitrogen) for 6h. Scale bar represents 4µm. (**D**) Quantification of Ste2-mEnvy mean fluorescent intensity at the plasma membrane in cells grown in SC media (+Nitrogen) or low nitrogen SC media (-Nitrogen) for 6h (n > 250 cells). Measurements were normalized to the mean of the -Nitrogen group to produce percentages. Error bars represent ±SEM. * = $p < 0.001$.

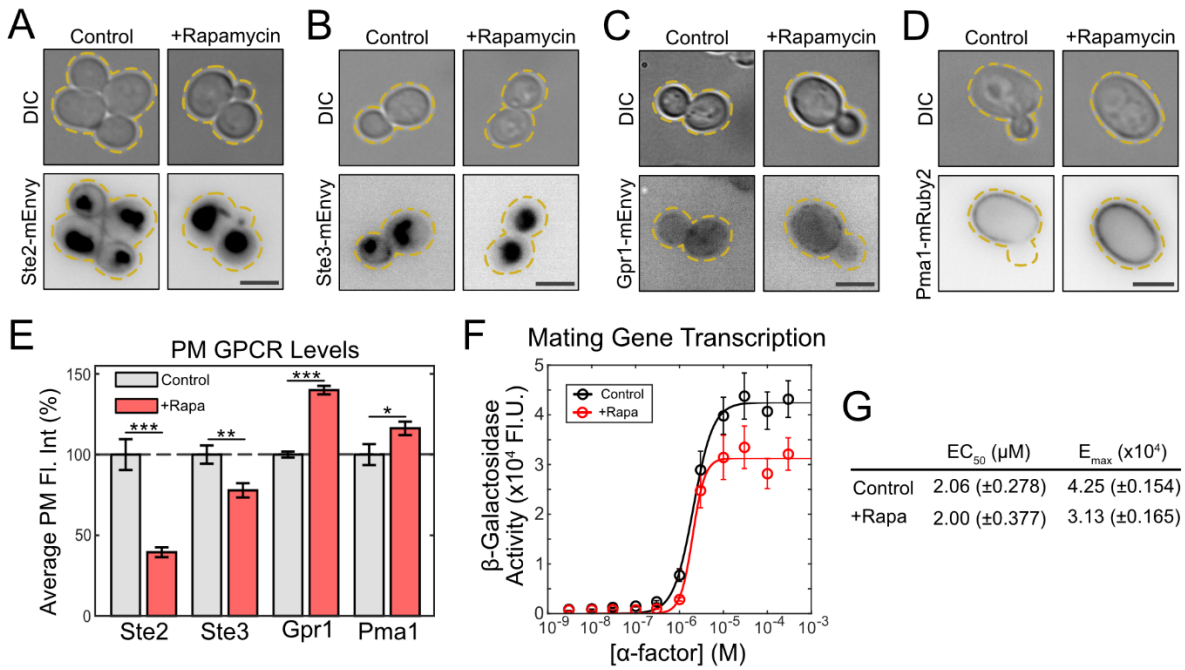

Fig. 2. TORC1 regulates GPCR association to the PM and dampens the mating pathway. (**A-D**) Representative images of cells expressing (**A**) Ste2-mEnvy, (**B**) Ste3-mEnvy, (**C**) Gpr1-mEnvy, and (**D**) Pma1-mRuby2 treated with or without 0.2μM rapamycin for 2h. Scale bars represent 4μm. (**E**) Quantification of Ste2-mEnvy (n > 200 cells), Ste3-mEnvy (n > 280 cells), Gpr1-mEnvy (n > 340 cells), and Pma1-mRuby2 (n > 250 cells) mean fluorescent intensities at the plasma membrane. Measurements were normalized to the mean of the untreated groups to produce percentages. Error bars represent ±SEM. * = $p < 0.05$, ** = $p < 0.01$, *** = $p < 0.001$. (**F**) β-galactosidase mating transcription assays of cell cultures treated with or without 0.2μM rapamycin for 2h (n > 10 colonies). Error bars represent ±SEM. (**G**) Table of EC_{50} and E_{max} responses to α-factor.

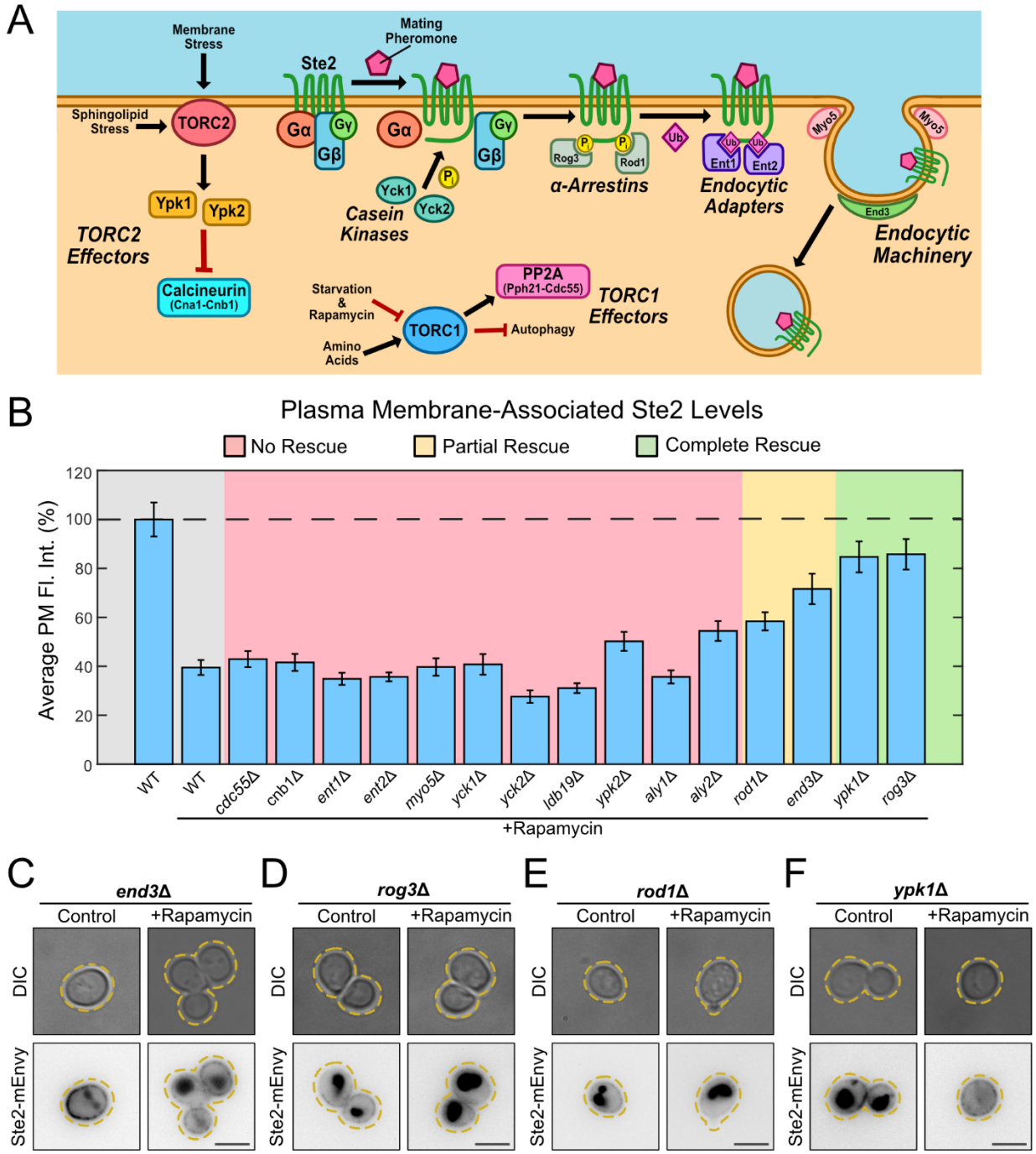

Fig. 3. TORC1-directed CME is mediated by α-arrestins and Ypk1. (**A**) To identify candidates involved in TORC1-mediated endocytosis, we deleted multiple genes that are involved in TORC signaling, receptor endocytosis, and CME. Casein kinases (*54-56*), α-arrestins (*25, 59*), and epsin-like proteins (*63, 64*) are all involved in priming the pheromone receptors for CME during mating. CME utilizes motors (*119*) and cytoskeletal organizers (*106, 107*) to form then endocytic pit that matures into an endosome. During starvation, TORC1 activity is reduced, downregulating PP2A activity (*120*). TORC2 activates Ypk1 and Ypk2 (*92, 96, 97*), which repress major cell regulators such as Calcineurin (*121*). (**B**) Quantification of Ste2-mEnvy mean fluorescent intensity at the plasma membrane in genetic mutants that do not express proteins

involved in TORC signaling, receptor endocytosis, and CME. These cells were treated with or without 0.2μM rapamycin for 2h ($n > 170$ cells). Measurements were normalized to the mean of the untreated groups (not shown excluding WT) to produce percentages. One-Way ANOVA was used to analyze variance between treated and untreated mutant and WT cells. Tukey's honest significance test was used as a multiple comparison test to compare means between groups. Based on ANOVA results, genetic mutants treated with rapamycin were grouped into one of three categories: 1) No Rescue (red), 2) Partial Rescue (Yellow), and 3) Complete Rescue. If the mean of the treated mutant was significantly lower ($p < 0.05$) than both untreated WT and mutant cells and were not significantly different from the treated WT cells, they were grouped into the "No Rescue" category. If the mean of the treated mutant was significantly lower than untreated mutant and WT cells and was significantly higher than treated WT cells, they were grouped in the "Partial Rescue" category. If the mean of the treated mutant was not significantly different from the untreated WT and mutant and was significantly higher than the mean of the treated WT cells, they were grouped into the "Complete Rescue" category. Error bars represent ±SEM. (**C-F**) Representative images of (**C**) *END*3Δ, (**D**) *ROG*3Δ, (**E**) *ROD*1Δ, and (**F**) *YPK*1Δ cells expressing Ste2-mEnvy. Scale bar represents 4μm.

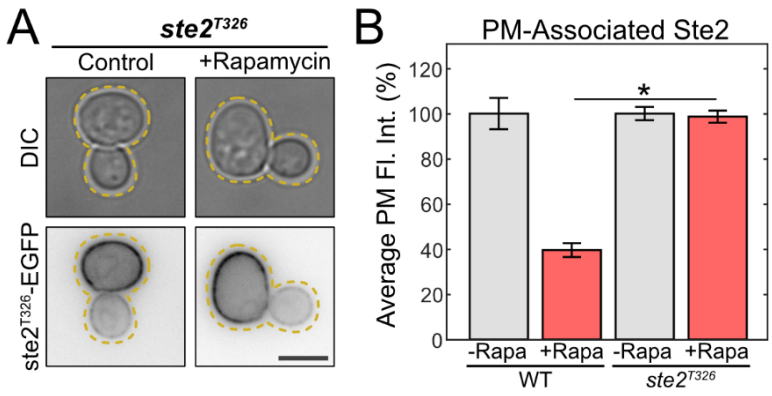

Fig. 4. The C-terminus of Ste2 is required for TORC1-mediated endocytosis. (**A**) Representative images of cells expressing Ste2^{T326}-EGFP treated with and without 0.2µM rapamycin for 2h. Scale bar represents 4µm. (**B**) Quantification of Ste2-mEnvy and Ste2^{T326}-EGFP (n > 130 cells) mean fluorescent intensities at the plasma membrane. Measurements were normalized to the mean of the untreated groups to produce percentages. One-Way ANOVA paired with Tukey's honest significance test was used to compare means between groups. Error bars represent ±SEM. * = $p < 0.001$.

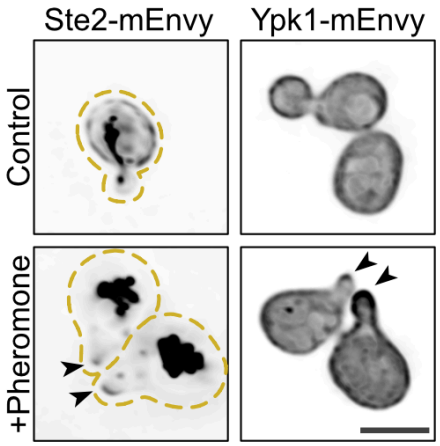

Fig. 5. Ypk1 localizes near Ste2 during the pheromone response. Representative images of Ste2-mEnvy and Ypk1-mEnvy in cells treated with and without 10µM α-factor. Images were corrected for hot and cold pixels and deconvolved through Huygens Essential 23.10 (Scientific Volume Imaging) using a measured point spread function, Classic MLE algorithm, SNR of 20, quality threshold of 0.01, and 500 max iterations. Images are max projections of deconvolution results for each strain and treatment. Scale bars represent 4µm.

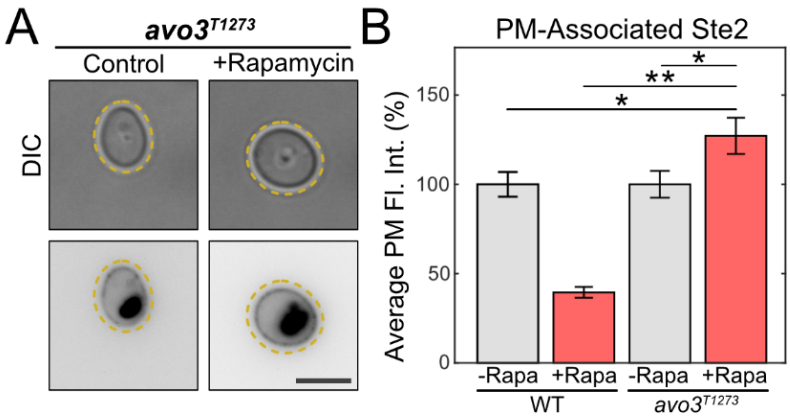

Fig. 6. TORC1-directed receptor endocytosis is mediated by TORC2. (**A**) Representative images of cells expressing Ste2-mEnvy and Avo3^{T1273} treated with and without 0.2µM rapamycin for 2h. Scale bar represents 4µm. (**B**) Quantification of Ste2-mEnvy (n > 130 cells) mean fluorescent intensities at the plasma membrane in cells with and without truncated Avo3. Measurements were normalized to the mean of the untreated groups to produce percentages. One-Way ANOVA paired with Tukey's honest significance test was used to compare means between groups. Error bars represent ±SEM. * = $p < 0.05$, ** = $p < 0.001$.

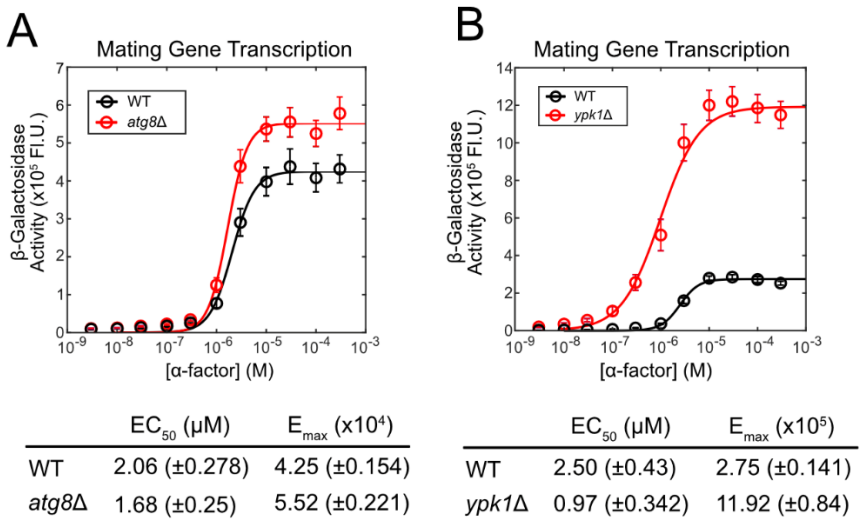

	EC_{50} (μM)	E_{max} (x10⁴)
WT	2.06 (±0.278)	4.25 (±0.154)
*atg8*Δ	1.68 (±0.25)	5.52 (±0.221)

	EC_{50} (μM)	E_{max} (x10⁵)
WT	2.50 (±0.43)	2.75 (±0.141)
*ypk1*Δ	0.97 (±0.342)	11.92 (±0.84)

Fig. 7. Pheromone-induced autophagy and Ypk1 dampens mating pathway output. (**A**) β-galactosidase mating transcription assays of WT and *ATG8*Δ cultures. Table of EC_{50} and E_{max} responses to α-factor in bottom panel. (n > 9 colonies). Error bars represent ±SEM. (**B**) β-galactosidase mating transcription assays of WT and *YPK1*Δ cultures. Table of EC_{50} and E_{max} responses to α-factor in bottom panel. (n = 9 colonies). Error bars represent ±SEM.

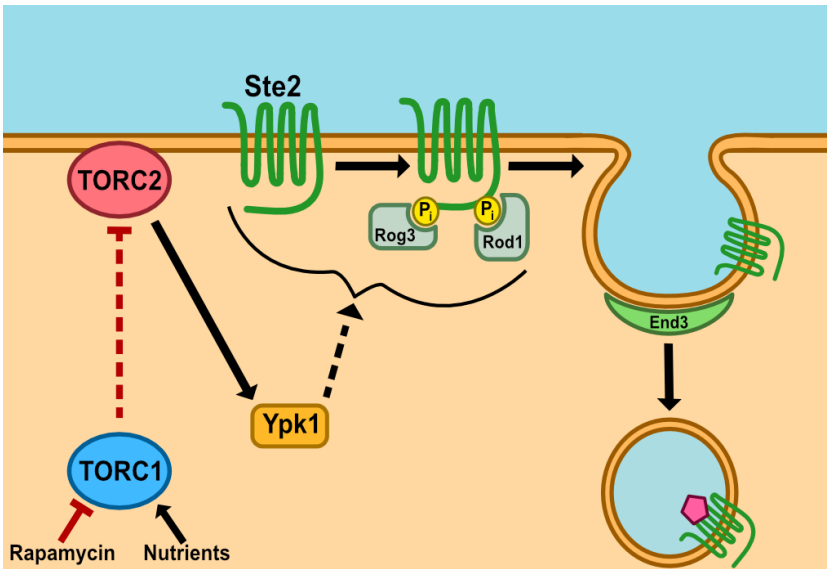

Fig. 8. Proposed mechanism of TORC1-directed endocytosis. In nutrient-deprived conditions, TORC1 is repressed, leading to the TORC2-directed activation of Ypk1. Active Ypk1 facilitates α-arrestin-directed CME of Ste2, which ultimately traffics to the vacuole.

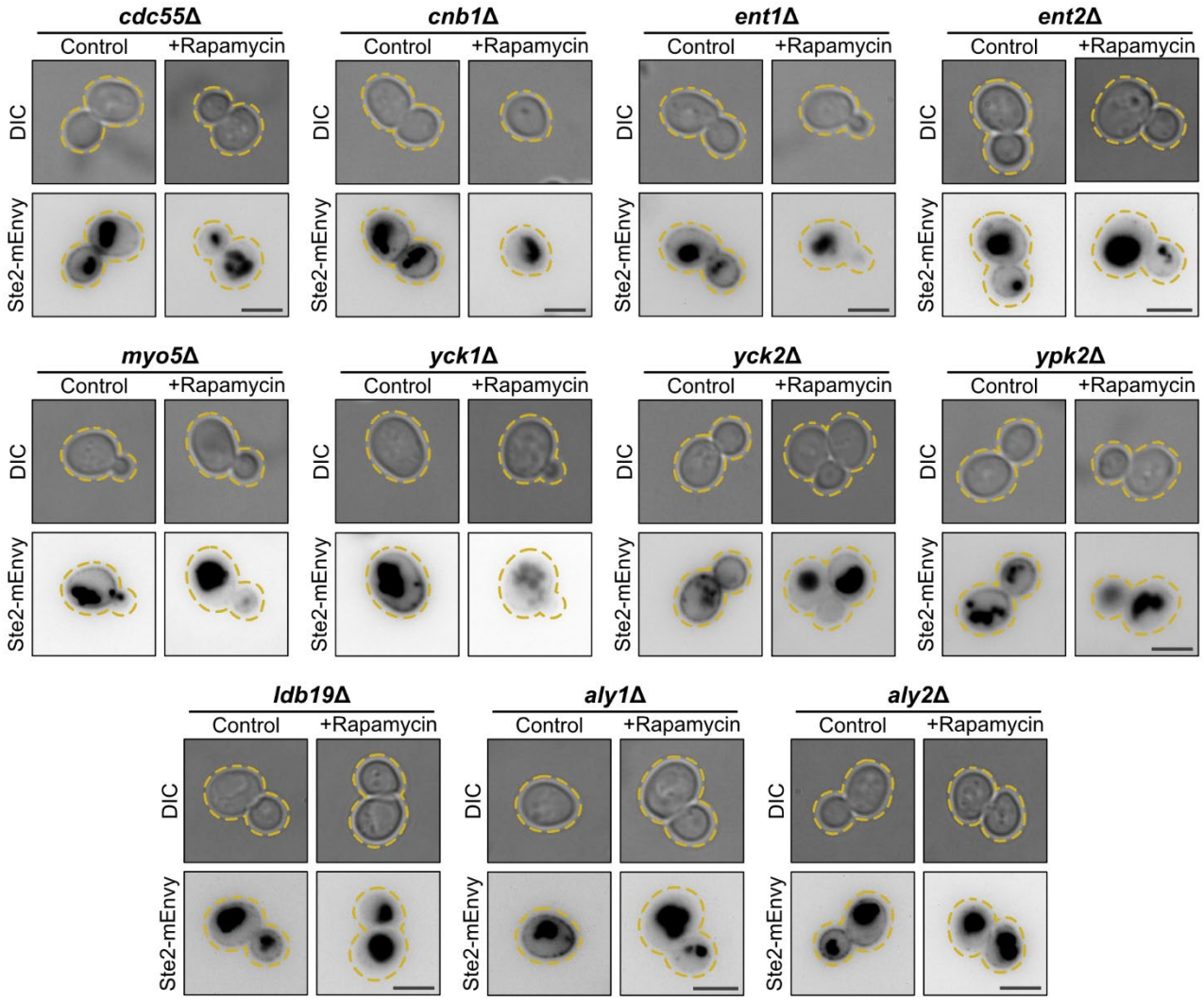

Figure S1. Single genetic deletions that do not block rapamycin-induced endocytosis. Representative images of genetic deletion mutants that do not block Ste2 internalization in the presence of 0.2μM rapamycin. Scale bars represent 4μm.

Table S1. Strain List.

Strain	***Parent***	***Description***
STE2-ENVY^{V206K}	BY4741	*STE2-ENVY^{V206K}::HIS3*
STE3-ENVY^{V206K}	BY4742	*STE3-ENVY^{V206K}::HIS3*
GPR1-ENVY^{V206K}	BY4741	*GPR1-ENVY^{V206K}::HIS3*
PMA1-mRUBY2	BY4741	*PMA1-mRUBY2::LEU2*
ATG8Δ	BY4741	*ATG8Δ::KanMX6*
STE2-ENVY^{V206K} ATG8Δ	BY4741	*STE2-ENVY^{V206K}::HIS3 ATG8Δ::KanMX6*
STE2-ENVY^{V206K} ALY1Δ	BY4741	*STE2-ENVY^{V206K}::HIS3 ALY1Δ::KanMX6*
STE2-ENVY^{V206K} ALY2Δ	BY4741	*STE2-ENVY^{V206K}::HIS3 ALY2Δ::KanMX6*
STE2-ENVY^{V206K} CDC55Δ	BY4741	*STE2-ENVY^{V206K}::HIS3 CDC55Δ::KanMX6*
STE2-ENVY^{V206K} CNB1Δ	BY4741	*STE2-ENVY^{V206K}::HIS3 CNB1Δ::KanMX6*
STE2-ENVY^{V206K} END3Δ	BY4741	*STE2-ENVY^{V206K}::HIS3 END3Δ::KanMX6*
STE2-ENVY^{V206K} ENT1Δ	BY4741	*STE2-ENVY^{V206K}::HIS3 ENT1Δ::KanMX6*
STE2-ENVY^{V206K} ENT2Δ	BY4741	*STE2-ENVY^{V206K}::HIS3 ENT2Δ::KanMX6*
STE2-ENVY^{V206K} LDB19Δ	BY4741	*STE2-ENVY^{V206K}::HIS3 LDB19Δ::KanMX6*
STE2-ENVY^{V206K} MYO5Δ	BY4741	*STE2-ENVY^{V206K}::HIS3 MYO5Δ::KanMX6*
STE2-ENVY^{V206K} ROD1Δ	BY4741	*STE2-ENVY^{V206K}::HIS3 ROD1Δ::KanMX6*

STE2-ENVY^{V206K} ROG3Δ	BY4741	*STE2-ENVY^{V206K}::HIS3 ROG3Δ::KanMX6*
STE2-ENVY^{V206K} avo3^{T1273}	BY4741	*STE2-ENVY^{V206K}::HIS3 avo3^{T1273}::KanMX6*
STE2-ENVY^{V206K} YCK1Δ	BY4741	*STE2-ENVY^{V206K}::HIS3 YCK1Δ::KanMX6*
STE2-ENVY^{V206K} YCK2Δ	BY4741	*STE2-ENVY^{V206K}::HIS3 YCK2Δ::KanMX6*
YPK1Δ	BY4741	*YPK1Δ::KanMX6*
YPK1-ENVY^{V206K}	BY4741	*YPK1-ENVY^{V206K}::KanMX6*
STE2-ENVY^{V206K} YPK1Δ	BY4741	*STE3-ENVY^{V206K}::HIS3 YPK1Δ::KanMX6*
STE2-ENVY^{V206K} YPK2Δ	BY4741	*STE2-ENVY^{V206K}::HIS3 YPK2Δ::KanMX6*
ste2^{T326}-EGFP	BY4741	*ste2^{T326}-EGFP::HIS3*

Table S2. Primer List.

Primer Name	***Sequence***	***Description***
WSM-7	5' ggaagccagaaagttctggactgaagataataataattta GGTGACGGTGCTGGTTTA 3'	Amplify fluorescent label to tag Ste2
WSM-8	5' gaaggtcacgaaattacttttcaaagccgtaaattttg ATCGATGAATTCGAGCTCG 3'	Amplify fluorescent label to tag Ste2
WSM-11	5' GATGCTAAAAGCAGTCTCAG 3'	Verify Ste2 labeling
WSM-12	5' GAGAGTTCTAGATCATGGCA 3'	Verify Ste2 labeling
NLM-1	5' cgaggtcgacggtatcgataCCAAAGGCTA AGGACGCTTTG 3'	Amplify *PMA1* ORF for Gibson Assembly
NLM-2	5' caccgtcaccGGTTTCCTTTTCGTGT TGAGTAG 3'	Amplify *PMA1* ORF for Gibson Assembly
NLM-3	5' aaaggaaaccGGTGACGGTGCTG GTTTAATTAAC 3'	Amplify *mRUBY2* ORF for Gibson Assembly
NLM-4	5' aaaagctggagctccaccgcTTACTTATACA ATTCATCCATACCACC 3'	Amplify *mRUBY2* ORF for Gibson Assembly
NLM-5	5' AAGCTCAAACGAACATAGTTCAGAAAATACTGC AGGCCCTGGTGACGGTGCTGGTTTA 3'	Amplify fluorescent label to tag Ste3
NLM-6	5' AATACTCCTAGTCCAGTAAATATAATGCGACACT CTTGTGTCGATGAATTCGAGCTCG 3'	Amplify fluorescent label to tag Ste3
NLM-7	5' CGGCATAGATTTGATAGCCTTCTTAAGAAATGG ACCATTAGGTGACGGTGCTGGTTTA 3'	Amplify fluorescent label to tag Gpr1
NLM-8	5' TTCCTTACTTTCCATTTTCAAACATCGCGATACA AAAACTTCGATGAATTCGAGCTCG 3'	Amplify fluorescent label to tag Gpr1
NLM-9	5' ACACCAATATCACAAGCGCA 3'	Verify Ste3 labeling
NLM-10	5' TCTGCTAATCGACTTTTGGAGC 3'	Verify Ste3 labeling
NLM-11	5' TCTACCCGGGTTGAAATTTGC 3'	Verify Gpr1 labeling
NLM-12	5' ACGAGCACTCATCCATTTTCA 3'	Verify Gpr1 labeling

NLM-15	5' AGAACCGACCAAGACGTGTT 3'	Amplify deletion cassette at *ATG8* ORF from Yeast Deletion Library
NLM-16	5' GTACGTTAAGAACAGCGGCA 3'	Amplify deletion cassette at *ATG8* ORF from Yeast Deletion Library
NLM-35	5' TCCCTCGTTCACAGAAAGTCT 3'	Verify Pma1 labeling
NLM-36	5' tgcatcacaggtccgttaga 3'	Verify Pma1 labeling
NLM-63	5' CCTTTTGATGTTACCCCGCC 3'	Amplify deletion cassette at *YCK1* ORF from Yeast Deletion Library
NLM-64	5' AAAGGGGCAAAGGTGTGAAG 3'	Amplify deletion cassette at *YCK1* ORF from Yeast Deletion Library
NLM-65	5' TCCACGTAGAACATCGCAGT 3'	Verify *YCK1* deletion
NLM-66	5' acaggaatcgaatgcaaccg 3'	Verify *YCK1* deletion
NLM-67	5' TCATTAAAGTGTGGGCTGTGG 3'	Amplify deletion cassette at *YCK2* ORF from Yeast Deletion Library
NLM-68	5' TGCAAATTGAAAGAGGGTAAACA 3'	Amplify deletion cassette at *YCK2* ORF from Yeast Deletion Library
NLM-69	5' GTCTTGATGCTCTGAAGGCG 3'	Verify *YCK2* deletion
NLM-70	5' tccgactcgtccaacatcaa 3'	Verify *YCK2* deletion
NLM-71	5' ACCAACAGTCCGCACATAGA 3'	Verify *YPK1* deletion and labeling
NLM-72	5' CCATGAGACACAAGCCACAC 3'	Verify *YPK1* deletion and labeling

NLM-79	5' AGTTCCTGTTTTGCCAATGGT 3'	Amplify deletion cassette at *MYO5* ORF from Yeast Deletion Library
NLM-80	5' GGAATTACCGACGCTCCATT 3'	Amplify deletion cassette at *MYO5* ORF from Yeast Deletion Library
NLM-81	5' TTGAGTTCTGCCGTTCAAGC 3'	Verify *MYO5* deletion
NLM-82	5' TAACGGCTCCAAGATTGTGC 3'	Verify *MYO5* deletion
NLM-83	5' TGGGTCAAATTATCGCGTATACAAATATACATA TAGTAACGACATGGAGGCCCAGAATAC 3'	Amplify deletion cassette with homology to *YPK2* UTRs
NLM-84	5' AAATTCCGTCCGGCTCGGCTCGGCTTGCTTCG GCTTGCTTCAGTATAGCGACCAGCATTC 3'	Amplify deletion cassette with homology to *YPK2* UTRs
NLM-85	5' TGGCGTGGTTGAACATCTTG 3'	Verify *YPK2* deletion
NLM-86	5' tccgactcgtccaacatcaa 3'	Verify *YPK2* deletion (with NLM-85), *ROD1* deletion (with RAM-15), and *ROG3* deletion (with RAM-17)
NLM-89	5' CCGATGAGGCAAAATATGGTGT 3'	Verify *ATG8* deletion
NLM-90	5' CGAACTCTTTCCCATTGTCTGT 3'	Verify *ATG8* deletion
NLM-91	5' GAGGGGTCAGAAGATGCAGA 3'	Amplify deletion cassette at *ALY1* ORF from Yeast Deletion Library
NLM-92	5' CCGGTACTTTTCCCAGACGA 3'	Amplify deletion cassette at *ALY1* ORF from Yeast Deletion Library
NLM-93	5' ATTCTGGGGAGGAGCAAGTC 3'	Verify *ALY1* deletion

NLM-94	5' CCAACCCGAGGAGAAATTGC 3'	Verify *ALY1* deletion
NLM-95	5' ACGCCTTCACCTATCACTCT 3'	Amplify deletion cassette at *ALY2* ORF from Yeast Deletion Library
NLM-96	5' GCGGGAAGAAGTCAAAAGACA 3'	Amplify deletion cassette at *ALY2* ORF from Yeast Deletion Library
NLM-97	5' GATGTCGAACGGAGAGCAAC 3'	Verify *ALY2* deletion
NLM-98	5' TTGGAACGGCTGAAGAAACG 3'	Verify *ALY2* deletion
NLM-99	5' CACATCAAGACCACTGCGAG 3'	Amplify deletion cassette at *CNB1* ORF from Yeast Deletion Library
NLM-100	5' AGATGGTCTGTCTCCTAGCA 3'	Amplify deletion cassette at *CNB1* ORF from Yeast Deletion Library
NLM-101	5' GGGAAATGGGTTGTGGACTT 3'	Verify *CNB1* deletion
NLM-102	5' AATCAGCGGGTTTCCTCCTT 3'	Verify *CNB1* deletion
NLM-107	5' AGCTCCACCTCAAAGACCAA 3'	Verify *CDC55* deletion
NLM-108	5' tccgactcgtccaacatcaa 3'	Verify *CDC55* deletion
NLM-111	5' GGAGAGATCTTACGCATAAAGAAATATAATATAG CGCACAGACATGGAGGCCCAGAATAC 3'	Amplify deletion cassette with homology to *CDC55* UTRs
NLM-112	5' GGGATAAAAAAAAGTAAGGGAAAATAAGGAATT ATTATAACAGTATAGCGACCAGCATTC 3'	Amplify deletion cassette with homology to *CDC55* UTRs
NLM-115	5' GTTCCTCTCATATCAACAAACATTAATACAGTTC CTGAAAGACATGGAGGCCCAGAATAC 3'	Amplify deletion cassette with homology to *YPK1* UTRs

NLM-116	5' TATGTCATGAGTAAACTAGTTGATAATGTATTCACTAAGTCAGTATAGCGACCAGCATTC 3'	Amplify deletion cassette with homology to *YPK1* UTRs
NLM-117	5' TACAATTTCTTTGTATACAGCGGGAAATTGACACTTCAAAGTTCCTCTCATATCAACAAA 3'	Extend homology of NLM-115/NLM-116 amplicon to *YPK1* UTR.
NLM-118	5' AGTAAGTAACGGAAAAGAAAACCTTTCTTTTATATAAAGTATGTCATGAGTAAACTAGT 3'	Extend homology of NLM-115/NLM-116 amplicon to *YPK1* UTR.
NLM-162	5' AGCGGATGGTCGTTCTTCTC 3'	Verify *END3* deletion
NLM-163	5' GCTGAAGCGTGAGAATGAGT 3'	Verify *END3* deletion
NLM-166	5' AAGCGATGGCGACTTGATAGAAAAATGCTTACCCATCTAGGACATGGAGGCCCAGAATAC 3'	Amplify deletion cassette to truncate *AVO3*
NLM-167	5' TTGTGACTATATACATTTATACATGCGGCCCTTTTTTGCTCAGTATAGCGACCAGCATTC 3'	Amplify deletion cassette to truncate *AVO3*
NLM-168	5' AGCCTTAGAAACCGACACGA 3'	Verify *AVO3* truncation
NLM-169	5' TCTGCTGAAACGGAACTCCC 3'	Verify *AVO3* truncation
NLM-189	5' TATTGGAAAGGCCGGTAAAGATAACAGGGATCTCTGAAAAGACATGGAGGCCCAGAATAC 3'	Amplify deletion cassette with homology to *END3* UTRs
NLM-190	5' AAATATTACACATTCATGTACATAAAATTAATTATCGGTGCAGTATAGCGACCAGCATTC 3'	Amplify deletion cassette with homology to *END3* UTRs
NLM-193	5' TATAATCAGACGATTGTAATATAACCATAGAGTTAGTGGGTATTGGAAAGGCCGGTAAAG 3'	Extend homology of NLM-189/NLM-190 amplicon to *END3* UTR.
NLM-194	5' TTCAAATCAAAAAAGTTTACAAGTGAAATAACAAACAGTAAATATTACACATTCATGTAC 3'	Extend homology of NLM-189/NLM-190 amplicon to *END3* UTR.

NLM-204	5’ ACAGCTAGGTAGCTCAATGGTGCAAGGTAGAAGCATTAGAGGTGACGGTGCTGGTTTA 3’	Amplify fluorescent label to tag Ypk1
NLM-205	5’ TATGTCATGAGTAAACTAGTTGATAATGTATTCACTAAGTTCGATGAATTCGAGCTCG 3’	Amplify fluorescent label to tag Ypk1
RAM-1	5’ CCCTACCCGACTGCAAACTA 3’	Amplify deletion cassette at *ROD1* ORF from Yeast Deletion Library
RAM-2	5’ TGTTGAGGAAGAAGTGCCAAG 3’	Amplify deletion cassette at *ROD1* ORF from Yeast Deletion Library
RAM-5	5’ GTTATGGACCCGGAGAGAGG 3’	Amplify deletion cassette at *ROG3* ORF from Yeast Deletion Library
RAM-6	5’ GTGTCGCAGTCCATAGAAGG 3’	Amplify deletion cassette at *ROG3* ORF from Yeast Deletion Library
RAM-9	5’ GGCCAGGTTGCTAGTGACTA 3’	Amplify deletion cassette at *LDB19* ORF from Yeast Deletion Library
RAM-10	5’ TGCCCACCCTTTATTTTGCC 3’	Amplify deletion cassette at *LDB19* ORF from Yeast Deletion Library
RAM-13	5’ ACCGTTGATGCTGATGAGGA 3’	Verify *LDB19* deletion
RAM-14	5’ CCCTCAAGCATCGCAGTTT 3’	Verify *LDB19* deletion
RAM-15	5’ CAAATCACTACAAGCCCGCA 3’	Verify *ROD1* deletion (with NLM-86)
RAM-17	5’ AGTATCGATGCGCTGAGTGA 3’	Verify *ROG3* deletion (with NLM-86)
SLM-3	5' TAGGCTTCTTACCGGCAGAG 3'	Amplify deletion cassette at *ENT1* ORF from Yeast Deletion Library

SLM-4	5' AGGACATGAGTACAGAGCACA 3'	Amplify deletion cassette at *ENT1* ORF from Yeast Deletion Library
SLM-5	5' AGATAGATGGCCGAACGTGG 3'	Amplify deletion cassette at *ENT2* ORF from Yeast Deletion Library
SLM-6	5' GACTCCAAAGGTGAATCTGGC3'	Amplify deletion cassette at *ENT2* ORF from Yeast Deletion Library
SLM-7	5' GGGAGAAGGAGTACCTTCTG 3'	Verify *ENT1* deletion
SLM-8	5' CCAGAATTATCTTTCGGGCC 3'	Verify *ENT1* deletion
SLM-10	5' CGAAGATGGCCGAATGATTGG 3'	Verify *ENT2* deletion
SLM-21	5' TGTGGGCATCTCTGGTTTGA 3'	Verify *ENT2* deletion
CJM-1	5' ACAACATCCACAGATAGGTTTTATCCAGGC ACGCTGTCTAGCGGTGACGGTGCTGGTTTA 3'	Amplify fluorescent label to tag and truncate Ste2
CJM-2	5' CGAAGGTCACGAAATTACTTTTTCAAAGC CGTAAATTTTGACGATGAATTCGAGCTCGTT 3'	Amplify fluorescent label to tag and truncate Ste2
CJM-3	5' CAATGTGGGCCACGGCTGCTAA 3'	Verify labeling and truncation of Ste2
CJM-4	5' ACAGCGTACCTTTAGACACGTGGG 3'	Verify labeling and truncation of Ste2
JKM-70	5' AACCCAATCTaagCTATCTAAAGACC 3'	Mutate Envy Val^{206} to Lys
JKM-71	5' GATAGGTAGTGGTTGTCTG 3'	Mutate Envy Val^{206} to Lys